Model Reduction in Physical Domain

by

Yong Ye

Submitted to the Department of Mechanical Engineering
in partial fulfillment of the requirements for the degree of

Ph.D. in Mechanical Engineering

at the

MASSACHUSETTS INSTITUTE OF TECHNOLOGY

February 2002

© Yong Ye, MMII. All rights reserved.

The author hereby grants to MIT permission to reproduce and
distribute publicly paper and electronic copies of this thesis document
in whole or in part.

ARCHIVES
MASSACHUSETTS INSTITUTE OF TECHNOLOGY
MAR 2 5 2002
LIBRARIES

Author .....
Department of Mechanical Engineering
September 1, 2001

Certified by .....
Kamal Youcef-Toumi
Professor
Thesis Supervisor

Accepted by .....
.....
Ain Sonin
Chairman, Department Committee on Graduate Students

Model Reduction in Physical Domain

by

Yong Ye

Submitted to the Department of Mechanical Engineering
on September 1, 2001, in partial fulfillment of the
requirements for the degree of
Ph.D. in Mechanical Engineering

Abstract

Modeling is an essential part of the analysis and the design of dynamic systems. Contemporary computer algorithms can produce very detailed models for complex systems with little time and effort. However, over complicated models may not be efficient. Therefore, reducing a model to a more manageable size has become an attractive research topic. A very useful type of reduced models is obtained by removing as many physical components as possible from the original model. Such approach is known as model reduction in the physical domain. Many results have been achieved in model reduction in the physical domain during past decades. Nonetheless, the newest developments in engineering practice as well as in theoretical research have brought about further challenges and opportunities. In this thesis, the criteria and the scope of model reduction in the physical domain are reinvestigated. As a result, a criterion based on the H_∞ norm of certain error model is proposed. Furthermore, the scope of model reduction is also extended. In this thesis, a mathematical framework is constructed for model reduction in physical domain. Specifically, model reduction problem is formulated as an optimization problem with bilinear matrix inequality (BMI) constraints. A branch-and-bound algorithm is developed to solve the BMI problem. The algorithm is proved to converge to global optimum. Several examples are presented to illustrate the use of the proposed model reduction scheme.

Thesis Supervisor: Kamal Youcef-Toumi
Title: Professor

Acknowledgments

I would like to thank my thesis advisor, Professor Kamal Youcef-Toumi for his advice and support. My Ph.D. program would not be the same without his knowledge, understanding and patience. I have had a very productive time with him.

I am also immensely grateful to my thesis committee members, Professor Haruhiko Asada, Professor Neville Hogan and Professor Alexandre Megretski. They have made extraordinary contribution to my thesis work. Furthermore, Professor Asada has provided me precious opportunities, academically and financially, via d'Arbeloff Home Automation and Healthcare Consortium under his leadership. Also, I have benefited tremendously from working for Professor Hogan, a caring supervisor and a insightful scholar, as a teaching assistant. And the professionalism of Professor Megretski has been a major driving force behind my research effort.

My thesis work is shaped with vital advice from many researchers. Among them are Professor Qingtai Ye of Shanghai Jiaotong University, Quanlin "Kate" Zhou, Isaac C. Kao and Bei Gu of MIT. Professor Masakazu Kojima and Mituhiro Fukuda of Tokyo Institute of Technology have provided me their BMI solver. In addition, I shall thank my colleagues at the Mechatronics Research Laboratory for their support.

This thesis is dedicated to my parents.

Contents

List of Figures

Chapter 1

Introduction

1.1 Motivations

Multi-energy domain dynamic systems are of great significance in contemporary industry. A multi-energy domain system may include mechanical, electrical, fluid and/or thermo components/subsystems [1]. Today such systems are involved in many aspects of our daily life. In traditional enterprises such as automobile industry, as well as at newly emerging frontiers such as home automation systems, engineers and researchers are working hard to find efficient means for the simulation, analysis and synthesis of these systems.

The rising importance of multi-energy domain systems has motivated intensive research activities on modeling methodologies. A multi-energy domain system usually contains a significant number of components. With the growing system complexity, the simulation, analysis and synthesis procedures rely increasingly on accurate and compact models, which in turn calls for systematic modeling procedures.

As a result of decades of enormous research effort and investment, detailed models for complex systems can now be built efficiently with various computer softwares. Such softwares include Simulink, Easy5 and 20Sim. New packages with more sophisticated features are also under development, including CASDA being programmed

[1] For the sake of succinctness from now on the word 'components' refers to both components and subsystems

at the Laboratory of Mechatronics Research at MIT. In fact, with the encapsulation function, which is available in virtually all successful modeling softwares, models with great complexity can be constructed in reasonable amount of time. Interestingly, it is this tremendous power of assembling complex models that brings about new challenges to the research of modeling methodology.

While complex models could be very accurate, they could also be unnecessarily cumbersome. Quite often not all the components make significant contribution to the system dynamic behavior[16]. Therefore, a vital step in modeling is to reduce the model to a more manageable size.

A very useful type of reduced models is obtained by removing as many physical components as possible from the original model. Such approach is known as model reduction in physical domain. The resultant models preserve the physical meanings of their structures and parameters, which are essential to analysis, synthesis and simulation. On analysis aspect, the information on physical structures and parameters provides insightful understanding toward how components contribute to system dynamic behavior. On synthesis aspect, such reduced model can be the basis of much simpler designs that achieve the performances of more complicated systems. On the simulation perspective, the resultant model may save considerable computational cost while providing meaningful data.

Attractive as this model reduction approach is, a systematic way to accomplish the task has been beyond the reach of researchers. During the past decade significant research efforts have been concentrated on this topic [1, 2, 3, 4, 5, 6, 7, 8, 11, 12, 18, 19, 20, 21, 22, 23, 24, 26, 35]. Section 1.2 gives a survey of existing procedures.

In this thesis, a methodic procedure is developed for model reduction in the physical domain. New concepts are incorporated into the development of the procedure, such as formulation of model reducion problem as an optimization problem. With these new concepts, and with contemporary mathematical tools, the proposed procedure has achieved some desirable properties, such as guaranteed convergence and guaranteed error bound.

The following sections give brief descriptions on existing as well as proposed model

reduction methods.

1.2 State of the Art

Currently, three major types of model reduction methods exist,

1. Methods based on the mathematical manipulation of a system's input-output relation,

2. Methods based on physical interpretation of system's dynamic behavior,

3. Combination of 1 and 2.

The first category, which has been developed mainly by control community [27, 28, 29, 30, 31, 32, 34, 57, 58, 59], include such procedures as modal truncation and balanced truncation. These procedures aim at reducing the order of the transfer matrix between the input and the output. One of their major advantages is that strict mathematical proofs exist. Furthermore, procedures such as balanced truncation target at worst case scenarios. Therefore the error bound of the reduced model is guaranteed. On the other hand, transfer matrices and their realizations are not designed to contain the information about the internal structure of the system. In general these procedures may not be directly applied to the modeling of physical systems.

The second category has been developed by mechanical engineering community [18, 19, 21, 24, 26]. This category includes various ad-hoc model reduction rules. Besides, in the past decade a family of procedures based on power criteria [2] have attracted significant amount of attention. These procedures try to identify the significance of a component by the magnitude of power flow associated with the component in a given dynamic process. These procedures have clear physical interpretations. However, such procedures are based on physical intuition rather than strict mathematical derivation. It is not surprising that in certain cases they can not guarantee error bounds.

[2]Power-based procedures are discussed in more details in Section 3.2.

The third category tries to combine the previous two categories and exploit the advantages of both [8, 9, 11, 12, 13, 22, 35]. The most prominent family of existing methods in this category are the MODA procedures[3] [22]. These methods are quite successful in dealing with simple dynamic systems or systems with some specific structure or parameter configurations. Examples of such systems include those of which the eigenvalues can be divided into several groups far away from one another on the s plane [8, 9, 11], or those of which the subsystems have very weak coupling with one another [11, 35]. The foundation of the procedures in this category is the understanding of the relation between system dynamics and system parameters and/or structure. Currently this relation is still far from fully comprehended, which is reflected by the fact the existing procedures are effective for relatively straight forward cases only. None the less, combining the mathematical and physical aspects of modeling is an interesting idea that attracts many researchers these days.

Although far from satisfactory, all these previous attempts have led to deeper understanding towards the behavior of dynamic systems. At the same time, a rich selection of powerful mathematical tools have become available in recent years. The utilization of up-to-date results from both physical and mathematical fields, along with the development of novel ideas, have made this thesis work possible.

1.3 Proposed Work

This thesis concentrates on model reduction of causal LTI lumped parameter systems with all eigenvalues in the open left half of the s plane. Specifically, the study focuses on removing independent energy storage elements. In this thesis 'removing' an energy storage element means setting the corresponding I or C to zero. Removing independent energy storage elements result in systems with lower orders, which facilitates a wide range of analysis, synthesis and simulation efforts.

On theoretical perspective, this thesis recalibrates the fundamentals of model reduction in physical domain and sets up a rigorous mathematical frame for the

[3]MODA procedures are discussed in more details in Section 3.3.

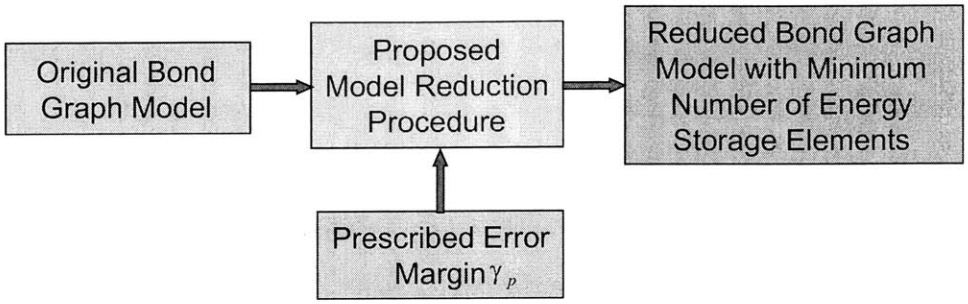

Figure 1-1: Outline of the Proposed Model Reduction Procedure

problem. Past works on the criteria as well as the scope of model reduction are reinvestigated. Based on the advantages and the restrictions of the past works, new concepts and solutions are proposed. Specifically, H_∞ norm of some error model is chosen to be a criterion for acceptable reduced models. At the same time, the scope of model reduction is expanded to include the adjustment of all system parameters in the process of finding a reduced model, as detailed in Chapter 4. These findings not only have clear physical meanings and rigorous mathematical definitions, but also paved a way for utilizing contemporary mathematical tools for solving model reduction problems. In fact, this thesis proposes the formulation of model reduction problem as an optimization problem with bilinear matrix inequality (BMI) constraints, and the solution constructed for the problem is proven to converge to global optimum.

On practical point of view, this thesis develops a fully automated algorithm with guaranteed error bound for model reduction in physical domain. Figure 1-1 gives an outline of the algorithm. Basically, the user supplies the original model and the acceptable error margin, the algorithm automatically searches for a reduced model with some energy storage element removed. Since rigorous mathematical formulation as well as proof for convergence are developed, for the type of problem discussed in this paper, as specified at the beginning of this section, the algorithm is guaranteed to provide the simplest model.

1.4 Thesis Outline

Chapter 1.2 gives a brief survey of existing model reduction procedures, including modal truncation, balanced truncation, optimal Hankel norm approximation, power approach and critical system eigenvalue approach.

Chapter 3 discusses the criteria for model reduction in the physical domain. The advantages and the disadvantages of two prominent criteria, namely the power criterion and the CSE criterion, are discussed. Furthermore, a criterion based on H_∞ norm of certain error model is presented. This criterion is the foundation of the work in this thesis.

Chapter 4 expands the scope of model reduction in the physical domain and sets up a mathematical formulation for the problem. Specifically, model reduction problem is extended to include appropriate change of system parameters. This is in contrast with most existing procedures, which try to eliminate some system components while keeping the parameters of the rest unchanged. It is shown that simpler models can be obtained with the extended model reduction problem. Furthermore, a parameterization scheme is found such that, with the help of positive definite lemma, the extended model reduction problem is formulated as an optimization problem under BMI constraints. BMI problems are among the most intensively studied topics nowadays. With the formulation proposed in this thesis up-to-date progresses in mathematical research can be applied to model reduction.

Chapter 5 presents a branch-and-bound based algorithm for solving the optimization problem associated with model reduction. A brief survey is given on the branch-and-bound method, followed by the construction of a branch-and-bound algorithm for model reduction problem. The proposed algorithm is shown to converge to global optimum.

Chapter 6 gives several examples to illustrate the proposed model reduction approach. The first example gives a graphic illustration of the convergence procedure of the branch-and-bound algorithm. The second example shows the proposed approach can achieve results that may be difficult to obtain with inspection. The third example

shows the use of a filter to specify the frequency range of interest, and the final one shows the application of the proposed procedure to model assembly problem.

Chapter 6 summarizes the contribution of the thesis and makes recommendations for further research.

Chapter 2

A Survey on Model Reduction Methods

This chapter presents a survey on existing model reduction methods. The methods to be reviewed include,

- Modal truncation
- Balanced truncation
- Optimal Hankel norm approximation
- Power approach
- Critical system eigenvalue approach

For each method, the following issues are discussed,

- What quantities are looked at in the model reduction procedure,
- To which systems the method is applicable,
- Which mathematical tools are used,
- What are the advantages and the disadvantages of the method.

2.1 Modal Truncation

The rational of modal truncation[17] identifies and removes the state variables associated with very fast modes. The method is applicable to LTI systems with some eigenvalues far away from the imaginary axis.

The method is based on the Jordan canonical form of the original system. For simplicity, assume that the original system has a set of unique eigenvalues[1] $\lambda_1, \ldots, \lambda_n$. In such a case, the Jordan canonical form of the system is,

$$\mathbf{A} = \begin{bmatrix} \lambda_1 & 0 & \ldots & 0 \\ 0 & \lambda_2 & \ldots & 0 \\ \vdots & \vdots & \ddots & \vdots \\ 0 & 0 & \ldots & \lambda_n \end{bmatrix} \mathbf{B} = \begin{bmatrix} b_1 \\ b_2 \\ \vdots \\ b_n \end{bmatrix} \mathbf{C} = \begin{bmatrix} c_1 & c_2 & \ldots & c_n \end{bmatrix} \tag{2.1}$$

Without loss of generality one can assume that $|\lambda_1| < |\lambda_2| < \ldots < |\lambda_n|$. The fastest eigenvalues are then removed with the corresponding state variables and the elements in $\mathbf{B}$ and $\mathbf{C}$.

The advantage of the modal truncation is that the poles of the truncated model are a subset of the poles of the original system. Therefore the method is quite useful for further analysis and/or design effort that are based on system spectrum. The disadvantage of the method is that the reduced model may not have a clear physical interpretation, due to the coordinate transform that is usually required to obtain the Jordan canonical form. Due to the coordinate transform, both the truncated and the preserved state variables are in general some combination of the state variables of the original system. And consequently it is difficult to determine which physical components are removed/kept in the reduced model.

[1] The result can be trivially extended to systems with repeated eigenvalues.

2.2 Balanced Truncation

The balanced truncation method[33] identifies and removes the state variables associated with small controllability/observability, in other words, the state variables that do not make significant contribution to the input/output relationship of the system. The method is applicable to LTI systems.

Balanced truncation is based on balanced realization of a transfer function[33]. A minimal realization $\mathbf{A}$, $\mathbf{B}$, $\mathbf{C}$ and $\mathbf{D}$ of a stable, rational transfer matrix $\mathbf{G}(s)$ is balanced if the controllability Gramian $\mathcal{P}$ and the observability Gramian $\mathcal{Q}$ satisfy,

$$\mathcal{P} = \mathcal{Q} = diag(\sigma_1, \sigma_2, \ldots, \sigma_n) \tag{2.2}$$

where $\sigma_1 \geq \sigma_2 \geq \ldots \geq \sigma_n$. $\mathcal{P}$ and $\mathcal{Q}$ can be calculated by solving the Lyapunov equations,

$$\mathbf{A}\mathcal{P} + \mathcal{P}\mathbf{A}^T + \mathbf{B}\mathbf{B}^T = 0 \tag{2.3}$$

$$\mathbf{A}^T\mathcal{Q} + \mathcal{Q}\mathbf{A} + \mathbf{C}^T\mathbf{C} = 0 \tag{2.4}$$

A standard procedure exists for obtaining balance realization. The procedure includes the following steps [33],

1. Compute the controllability and observability Gramians $\mathcal{P}$ and $\mathcal{Q}$.
2. Find a matrix $\mathcal{R}$ such that $\mathcal{P} = \mathcal{R}^*\mathcal{R}$.
3. Diagonalize $\mathcal{R}\mathcal{Q}\mathcal{R}^*$ to get $\mathcal{R}\mathcal{Q}\mathcal{R}^* = \mathcal{U}\mathbf{\Sigma}^2\mathcal{U}^*$.
4. Let $\mathcal{T}^{-1} = \mathcal{R}^*\mathcal{U}\mathbf{\Sigma}^{-1/2}$. Then $(\mathcal{T}\mathcal{A}\mathcal{T}^{-1})$, $\mathcal{T}\mathcal{B}$, $\mathcal{C}\mathcal{T}^{-1}$, $\mathcal{D}$ is a balance realization.

A reduced model with lower system order can be obtained with the truncation of the balance realization. Specifically, let the balanced realization $\mathcal{A}$, $\mathcal{B}$, $\mathcal{C}$ and $\mathcal{D}$ of $\mathbf{G}(s)$ and the corresponding $\mathbf{\Sigma}$ be partitioned compatibly as,

$$\mathcal{A} = \begin{bmatrix} \mathcal{A}_{11} & \mathcal{A}_{12} \\ \mathcal{A}_{21} & \mathcal{A}_{22} \end{bmatrix}$$

$$\begin{aligned} \mathcal{B} &= \begin{bmatrix} \mathcal{B}_1^T & \mathcal{B}_2^T \end{bmatrix}^T \\ \mathcal{C} &= \begin{bmatrix} \mathcal{C}_1 & \mathcal{C}_2 \end{bmatrix} \\ \mathbf{\Sigma} &= \begin{bmatrix} \mathbf{\Sigma}_1 & \mathbf{0} \\ \mathbf{0} & \mathbf{\Sigma}_2 \end{bmatrix} \end{aligned} \tag{2.5}$$

where the smallest eigenvalue of $\mathbf{\Sigma}_1$ is greater than the largest eigenvalue of $\mathbf{\Sigma}_2$. Then the system $\hat{\mathbf{G}}$ defined by $\mathcal{A}_{11}$, $\mathcal{B}_1$, $\mathcal{C}_1$ and $\mathcal{D}$ is stable, and $\|\mathbf{G}(s) - \hat{\mathbf{G}}(\mathbf{s})\|_\infty \leq 2trace(\mathbf{\Sigma}_2)$. Often Σ_1 and Σ_2 are chosen such that the summation of all components of Σ_2 is much less than the smallest component of Σ_1.

Balanced truncation procedure is very successful. This is partly due to the fact that it provides a systematic method for achieving a reduced order transfer matrix and guarantee the error of the reduced model in H_∞ norm. On the other hand, the procedure is not designed for model reduction in physical domain. In the similarity transform with $\mathcal{T}$, the physical meaning of the resultant state space realization may be lost, and may be difficult to recover after the truncation. Consequently, very few publication have been seen on the application of balanced truncation in physical domain. One of these few works is Reference [12], in which balanced truncation is used to estimate the order and the spectrum of the reduced model before some model reduction in physical domain is performed.

2.3 Optimal Hankel Norm Approximation

Similar to the balanced truncation method, the optimal Hankel norm approximation method[60] identifies and removes the state variables associated with small controllability/observability. The method is applicable to LTI systems.

With optimal Hankel norm approximation, one tries to progressively remove the state variables associated with the smallest Hankel singular number. To remove the such state variables, one shall use the following steps[60],

1. Find a balanced realization $\mathcal{A}$, $\mathcal{B}$, $\mathcal{C}$, $\mathcal{D}$ with

$$\mathbf{\Sigma} = \begin{bmatrix} \mathbf{\Sigma}_1 & 0 \\ 0 & \sigma \mathbf{I}_r \end{bmatrix} \tag{2.6}$$

where σ is the smallest Hankel singular number of the transfer matrix $\mathbf{G}(s)$ and r is the multiplicity of σ.

2. Partition $\mathcal{A}$, $\mathcal{B}$ and $\mathcal{C}$ according to the partition of **Sigma**,

$$\begin{aligned} \mathcal{A} &= \begin{bmatrix} \mathcal{A}_{11} & \mathcal{A}_{12} \\ \mathcal{A}_{21} & \mathcal{A}_{22} \end{bmatrix} \\ \mathcal{B} &= \begin{bmatrix} \mathcal{B}_1^T & \mathcal{B}_2^T \end{bmatrix}^T \\ \mathcal{C} &= \begin{bmatrix} \mathcal{C}_1 & \mathcal{C}_2 \end{bmatrix} \end{aligned} \tag{2.7}$$

and find an orthogonal matrix $\mathbf{U}$ such that $\mathbf{B}_2 = -\mathbf{C}_2^T\mathbf{U}$.

3. Construct the state space matrices of the reduced system by,

$$\hat{\mathbf{A}} = \mathbf{\Gamma}^{-1}(\sigma^2\mathcal{A}_{11}^T + \mathbf{\Sigma}_1\mathcal{A}_{11}\mathbf{\Sigma}_1 - \sigma\mathcal{C}_1^T\mathbf{U}\mathcal{B}_1^T) \tag{2.8}$$

$$\hat{\mathbf{B}} = \mathbf{\Gamma}^{-1}(\mathbf{\Sigma}_1 + \sigma\mathcal{C}_1^T\mathbf{U}) \tag{2.9}$$

$$\hat{\mathbf{C}} = \mathcal{C}_1\mathbf{\Sigma}_1 + \sigma\mathbf{U}\mathcal{B}_1 \tag{2.10}$$

$$\hat{\mathbf{D}} = \mathcal{D} - \sigma\mathbf{U} \tag{2.11}$$

where $\mathbf{\Gamma} = \mathbf{\Sigma}_1^2 - \sigma^2\mathbf{I}$.

The advantage of the optimal Hankel norm approximation is that it has a even smaller error bound than the balanced truncation. Reference [60] states that the transfer matrix of the reduced model, $\hat{\mathbf{G}}(s)$, satisfies $\|\mathbf{G}(s) - \hat{\mathbf{G}}(s)\|_\infty = \sigma$, while if balanced truncation was used one would have $\|\mathbf{G}(s) - \hat{\mathbf{G}}(s)\|_\infty = 2r\sigma$. However, the potentially higher accuracy comes with the cost of more involved mathematical calculation. At the same time, the method shares the disadvantage of the balanced

truncation, which is the lack of physical interpretation due to the similarity transform required to obtain the balanced realization in step 1.

2.4 Power Approach

The power approach[19, 26] stipulates that the physical components that are associated with small power flows make insignificant contribution to the overall system dynamic behavior. The approach is used on lumped parameter systems.

The approach uses numerical simulation to obtain the power flow associated with the system's dynamic behavior under certain specific input(s), and remove the component(s) with small power flow. A detailed presentation of the method can be found in the next chapter.

The advantage of the method is that it has very straightforward physical interpretation. Also, the method does not involve the use of high level mathematical concepts, which makes it readily acceptable to most engineers in industry. On the other hand, as shown in the next chapter, power associated with a physical component is not a good criterion to measure the significance of the component, and the power approach may lead to erroneous results.

2.5 Critical System Eigenvalue Method

The critical system eigenvalue method[25] identifies and removes the physical component(s) that make insignificant contribution to a prescribed set of system eigenvalues, called critical system eigenvalues. It is applicable to LTI systems.

This method uses two stages of exhausted search to identify the relevant physical component(s). A more detailed presentation of the method can be found in the next chapter.

The advantage of the procedure includes its clear physical meaning. Also the critical eigenvalues of the original system and the reduced system are close to each other, which is a very desirable property. A major disadvantage is the low efficiency

Chapter 3

Criteria for Model Reduction in Physical Domain

3.1 Introduction

This chapter examines some widely used criteria for model reduction in the physical domain and proposes a criterion used in this thesis. The choice of a criterion is essential for a sound reduction procedure. To a large extent, the criterion determines both the usefulness and the computational cost of the model reduction procedure. An ideal criterion should use value(s) with clear physical meaning, to sufficiently describe the error of a prospective reduced model. At the same time, efficient methods should be available for calculating this value. Section 3.2 discusses the power criteria, which have been widely used for model reduction in the physcial domain during the past decade [18, 19, 21, 24, 26]. Three counter examples are presented for these criteria. Section 3.3 discusses the critical system eigenvalue criterion [20, 22, 25], another popular criterion. Section 3.4 proposes a criterion based on the H_∞ norm of a certain error model. The physical meaning of the criterion is presented as well. As shown later, H_∞ criterion lays the foundation of a more general, more rigorous and more computationally effective model reduction procedure.

3.2 Power Criteria

In the past decade, a very active research area of model reduction in the physical domain is a family of procedures based on power criteria [18, 19, 21, 24, 26]. The underlying intuition of the power criteria is the conjecture that components associated with small power flow makes small contribution to a system's dynamic behavior. The existing model reduction approaches based on power criteria are composed of the following three major steps,

1. Calculate a system's time response under certain input with numerical simulation,

2. Use various indices to measure the power flow into and/or out of a component,

3. Remove the components associated with low power flow level.

However, despite of more than ten years of research, no strict mathematical proof has been presented for the conjecture. The lack of a proof has prompted the author to reinvestigate such criteria and come up with several counter examples.

This section shows that the use of the power criteria may lead to erroneous results. Three examples are presented,

1. Elements associated with low power flow may make large contribution to the system dynamic behavior,

2. Elements associated with high power flow may make small contribution to the system dynamic behavior,

3. Elements associated with low power flow for one input direction may have high power flow for another.This adds further trouble for power criteria, which rely on the systems' time response to specific inputs. Because calculating the time response for all possible input directions is impractical.

The power criteria use various time averages of the power flow associated with a component to measure the corresponding power level. As pointed out in reference

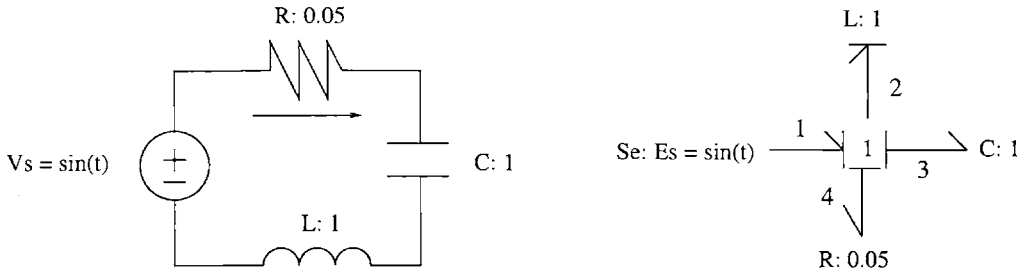

Figure 3-1: Contribution of an Element with Low Power Level

[18], the power flow of a component is in general a function of time. For example, if the current goes through a resistant R is $sin(t)$, then the power flow into the resistant is $Rsin^2(t)$. The researchers using power criteria [18, 24] believe that various time averages can used as the measurements for the power flow level associated with a component. In literatures [18, 19, 21, 24, 26], two different indices have been used. One is the RMS metric, which is the square root of the time average of the square of the power flow. Specifically, RMS metric is defined as $\mathcal{P}_i = \sqrt{\frac{1}{T}\int_0^T P_i^2(t)dt}$ where $P_i(t)$ is the power associated with bond i. The other is the activity index defined as $AI_i = \frac{\int_0^T |P_i(t)|dt}{\sum_{j=1}^{n}\int_0^T |P_i(t)|dt}$, where n is the total number of bonds in a bond graph model. Activity index is the normalized time average of the absolute value of power flow.

The example in Figure 3-1 demonstrates that an element associated with low power level can make a significant contribution to the system dynamic behavior. The physical system is composed of a voltage source, a resistance, a capacitance and a inductance. Suppose the output of the system is the flow associated with the 1 junction, which is the current in the circuit. Also, let the initial conditions be zero. Since this system is of second order, analytical solution of the time response can be calculated. With the notations in Figure 3-1 and denote the output current be $i(t)$, the system dynamic equation can be written as,

$$\frac{di^2(t)}{dt^2} + \frac{R}{L}\frac{di(t)}{dt} + \frac{1}{LC}i(t) = \frac{1}{L}\frac{dsin(t)}{dt} \tag{3.1}$$

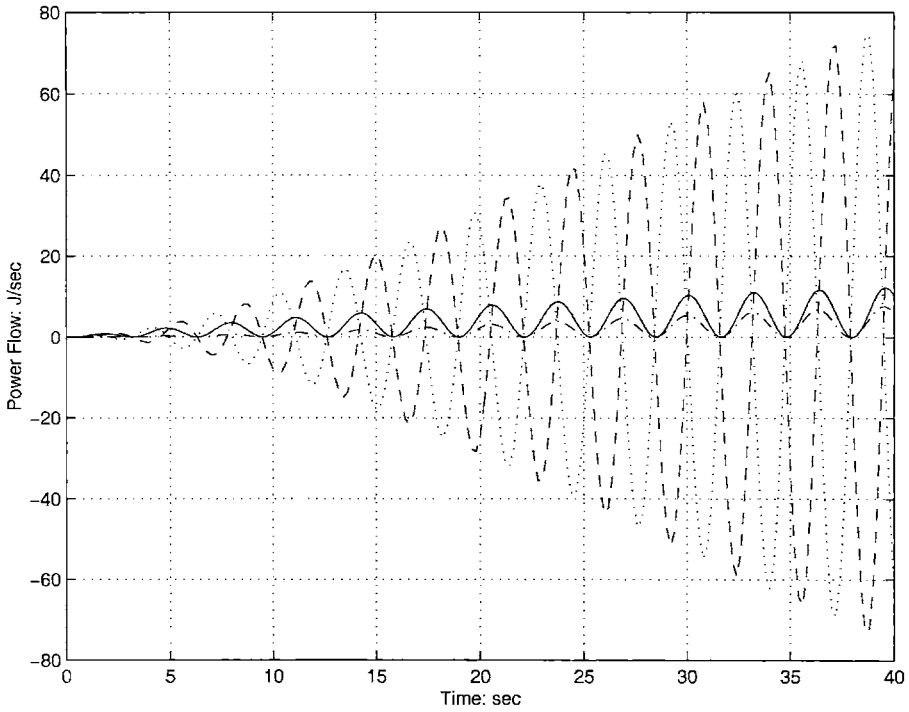

Figure 3-2: Power v.s. Time: Solid: Se (Bond 1), Dotted: L (Bond 2), Dashed: C (Bond 3), Dash-Dotted: R (Bond 4)

Following any standard procedure for solving second order systems, $i(t)$ can be obtained as,

$$i(t) = 20sin(t) - 20.0062e^{-0.0025t}sin(0.9997t) \tag{3.2}$$

At the same time, the voltage across the inductance V_L, the capacitance V_C and the resistance V_R, which are useful for calculating the power flow associated with each component, can be obtained as $V_L = L\frac{di(t)}{dt}$, $V_C = \int_{\tau=0}^{t} i(\tau)d\tau$ and $V_R = Ri(t)$ respectively. Finally the power flow associated with each component is the multiplication of the flow and the voltage associated with the component. The calculated power responses of the components are shown in Figure 3-2. The RMS of the power associated with the bonds 1, 2, 3, 4 are $\mathcal{P}_1 = 5.0408, \mathcal{P}_2 = 28.6864, \mathcal{P}_3 = 29.0632$ and $\mathcal{P}_4 = 2.5939$

respectively [1]. Obviously $\mathcal{P}_4$ is significantly smaller than the others. Thus according to the RMS index, bond 4 and therefore element R can be removed. Also, one can calculate the activity indices as $AI_1 = 0.0781, AI_2 = 0.4399, AI_3 = 0.4461$ and $AI_4 = 0.0359$. The activity index of bond 4 is obviously the smallest and significantly smaller than all the others. So the activity indices also indicates that bond 4 can be removed. Now Figure 3-3 plots the flow of the original model and that of the reduced model[2]. In this figure at $t = 39.4sec$, for the original model $i(39.4) = 12.2628$, but for the reduced model $i(39.4) = 19.3674$. The error is 58%, which is significant. Therefore, the R element is relevant to the flow associated with the 1 junction. The physical meaning of this result is now interpreted. In the time interval $[20sec, 40sec]$, the R element dissipates about half of the power supplied by the source. Also note that the dissipated power is on average less than one tenth of the power being exchanged between the I and C element. By eliminating the R element, the rate of increase of the energy in the system is changed significantly. Therefore with the increase of time the error increases slowly but steadily.

The example in Figure 3-4 shows the case where the elements with high power level make insignificant contribution to the system dynamic behavior. The input is $f_s = 0$. Suppose the output is the flow associated with m_1 and the spring displacements have the initial values of $x_{k1}(0) = 1$ and $x_{k2}(0) = 0.015$. The simulated power responses of the components are shown in Figure 3-5. The RMS power of the bonds are: $\mathcal{P}_1 = 0, \mathcal{P}_2 = 0.3497, \mathcal{P}_3 = 0.4464, \mathcal{P}_4 = 0.8096, \mathcal{P}_5 = 0.7308, \mathcal{P}_6 = 1.5808$ and $\mathcal{P}_7 = 1.7443$. Thus according to the RMS index, k_2 and m_2 are the most important elements in the system. The activity indices are found to be $AI_1 = 0, AI_2 = 0.0655, AI_3 =$

[1] One may observe that $\mathcal{P}_2$ and $\mathcal{P}_3$ are greater than $\mathcal{P}_1$. This is not surprising because of the resonant behavior of this lightly-damped second order system. In fact, this system has damping coefficient $\xi = 0.025$, natural frequency of $\omega_n = 1rad/sec$ and damped natural frequency of $\omega_d = 0.9997$. Due to the small damping ratio one can expect a very high resonant peak. And since the input frequency is very close to the damped natural frequency, the system gets very close to resonant peak. For lightly-damped system being excited close to resonant frequency, the time average of power associated with energy storage elements can be greater than the power input to the system.

[2] One may notice that in this example the period of the original system is longer than that of the reduced model. This is because the original system has damping, so in the transient period one can observe the oscillation at damped natural frequency, which is lower than the natural frequency as observed in the reduced model, which does not have damping.

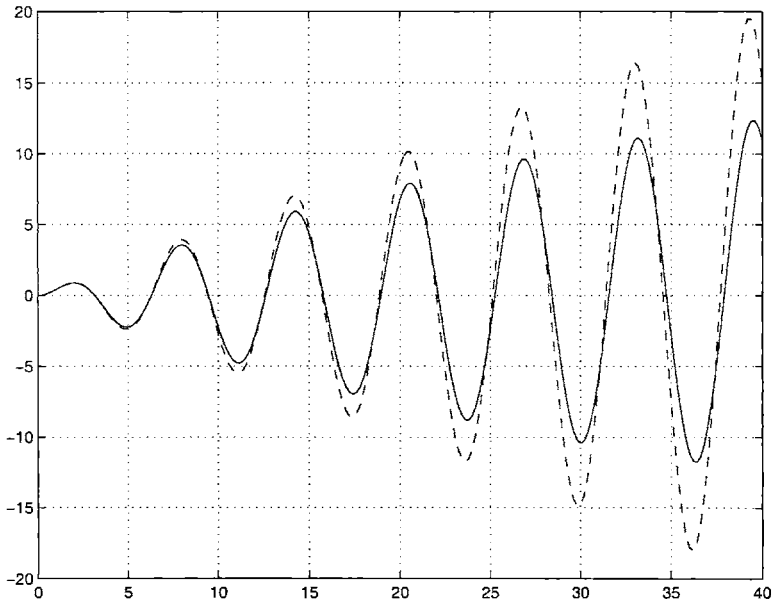

Figure 3-3: Flow of 1 Junction: Solid: Original Model, Dashed: Reduced Model

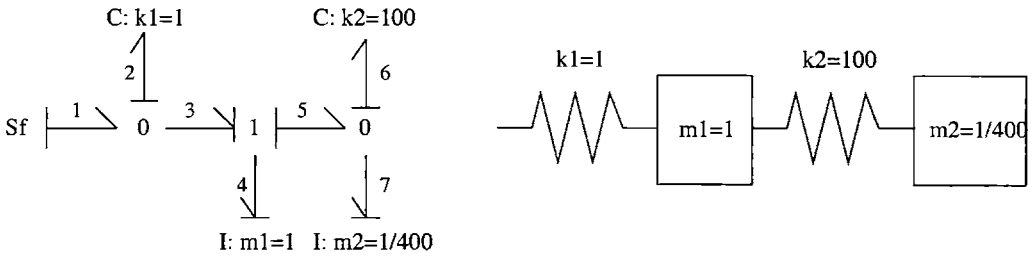

Figure 3-4: Contribution of an Element with High Power / Energy Level

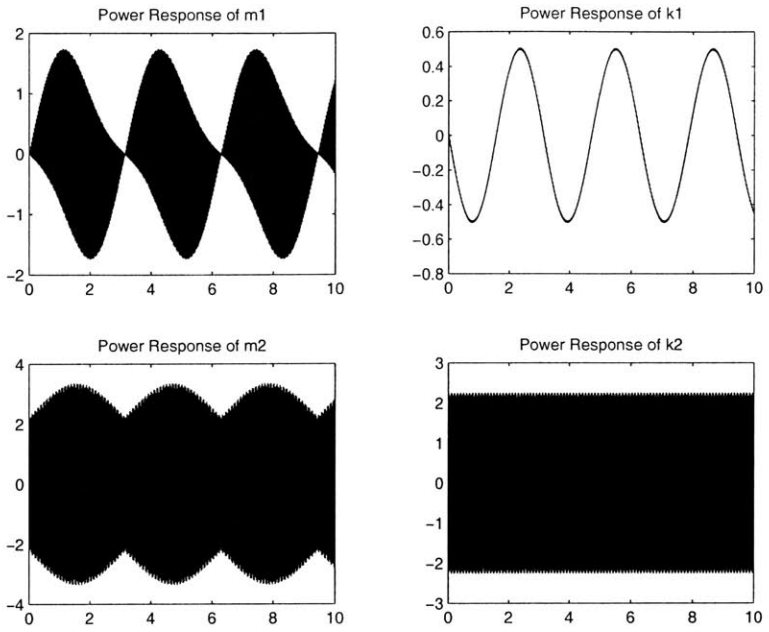

Figure 3-5: Simulation of power v.s. time

$0.0697, AI_4 = 0.1318, AI_5 = 0.1223, AI_6 = 0.2979, AI_7 = 0.3128$, which also indicates that bond 6 and bond 7, and correspondingly k_2 and m_2, are important. Now consider a reduced system with bond 6 and 7 removed along with k_2 and m_2. Bond 5 is therefore also eliminated since the 0 junction it connects becomes isolated without bonds 6 and 7. Figure 3-6 shows the output of the original system and that of the reduced system. The two curves are indistinguishable. In this example, one can see that the dynamics of the subsystem consists of k_2 and m_2 is much faster than that of the rest of the system. Although the magnitude of the power associated with bond 5 is large, its direction switches in such a short time, that the subsystem composed of bond 1 through 4 hardly feels the existence of bond 5. Therefore, the k_2 and m_2 elements are not relevant.

The third example shows that for different input directions the power flow associated with a component can be very different, and therefore power criteria, which are based on the power flow associated with individual components under specific inputs, may not be useful for MIMO systems. Consider a two-input system with a transformer. The physical system and the corresponding bond graph model are shown in

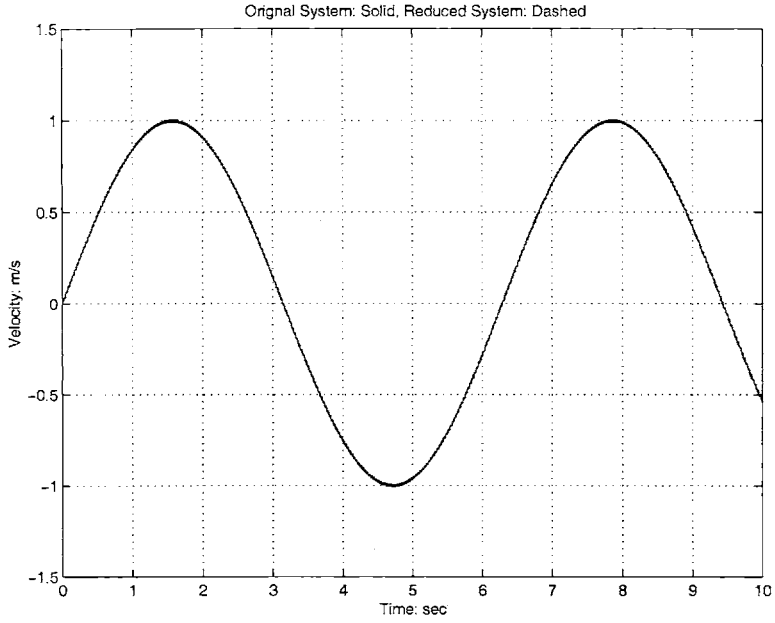

Figure 3-6: Output: Original System v.s. Reduced System

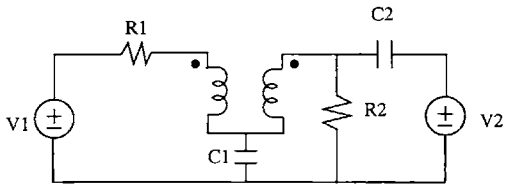

Physical System

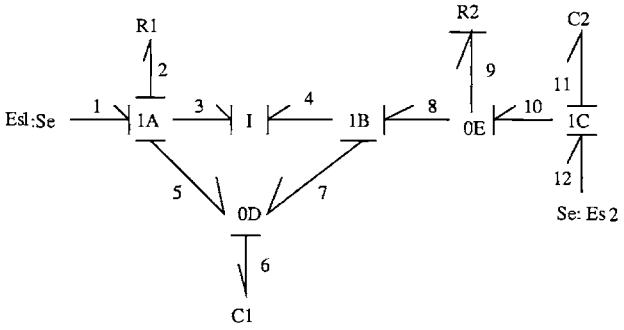

Bond Graph Model

Figure 3-7: An MIMO System

Figure 3-7. The system parameters are: $R_1 = 0.7, R_2 = 10, C_1 = 5, C_2 = 50$, and the constitutive relation of the I field is,

$$\begin{bmatrix} f_3 \\ f_4 \end{bmatrix} = \begin{bmatrix} 4 & -8 \\ -8 & 36 \end{bmatrix} \begin{bmatrix} p_3 \\ p_4 \end{bmatrix} \tag{3.3}$$

where f_i and p_i represent the flow and the momentum associated with the i^{th} bond respectively. Let the effort $e_6(t)$ associated with the capacitance C_1 be the output. Following standard procedures in system analysis, the transfer matrix relating $E_6(s)$ and the input vector $\mathbf{U(s)} = [V_1(s), V_2(s)]^T$ can derived,

$$E_6(s) = \mathbf{G}(s)\mathbf{U}(s) = \frac{1}{g_0} \begin{bmatrix} g_1 & g_2 \end{bmatrix} \mathbf{U}(s) \tag{3.4}$$

where

$$g_0 = s^4 + 7.8s^3 + 1934s^2 + 3680s + 2.14e004 \tag{3.5}$$

$$g_1 = -20s^2 - 100s + 2e004 \tag{3.6}$$

$$g_2 = 140s^2 + 280s - 7.399e - 012 \tag{3.7}$$

Figure 3-8 shows the plot of the singular values of $\mathbf{G}$ versus frequency. Only one curve is visible since at any frequency, the smaller one of the singular values is zero. As seen in the plot, the magnitude of the effort associated with the capacitance C_1 changes significantly, from zero corresponding to σ_{min} to 1.75 corresponding to σ_{max} at $3.032 rad/sec$, depending on the input direction. In fact, at this frquency for the input direction corresponding to the larger singular value, the circuit displays a resonant behavior and therefore both of the indices of the power flow goes in/out of C_1 are large. More detailed computation shows that the power criteria indicate the component of C_1 is important for the input directions associated with largest singular values while irrelevant for those associated with zero singular value. In short, the conclusion drawn for one input direction can not be generalized for another.

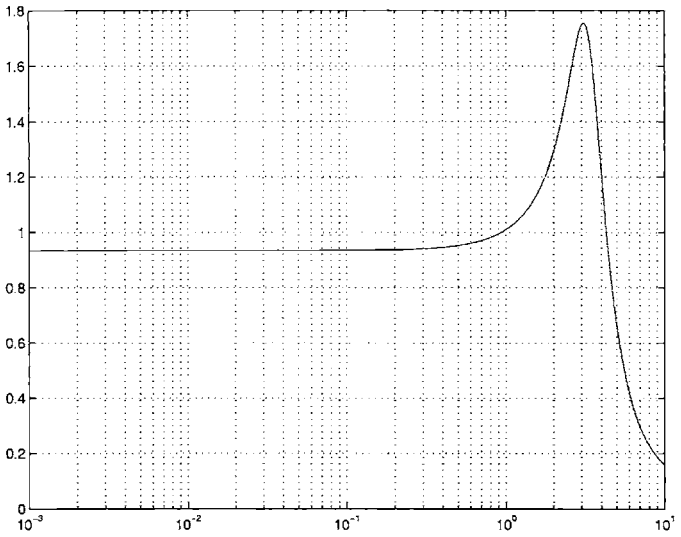

Figure 3-8: Singular Value v.s. Frequency

The counter examples in this section show that the power criteria, as they are defined up to now, have severe limitations.

3.3 Critical System Eigenvalue Criterion

Another criterion for model reduction in physical domain is the critical system eigenvalue criterion [20, 22, 25]. Intuitively, this criterion requires that the eigenvalues of the reduced model be close to those of the original model within a semi-circle of a prescribed radius on the left half of the s plane.

Up to this time, the only procedures that that implement critical system eigenvalue criterion are the MODA procedures. The MODA procedure most related to model reduction of LTI systems in physical domain was published in [22] and is discussed here. This procedure includes two stages[3]. The first stage is to determine the 'critical system eigenvalues', denoted as CSEs in [22]. The CSEs are constructed by progressively increase the complexity of a candidate model till its spectrum radius reaches a

[3]The fact that the MODA procedure is repeated here does not mean the author agrees with all the implicit assumptions Reference [22] made for this procedure, neither does it mean the author agrees with the underlying thoughts of the procedure.

prescribed value. This spectrum radius is named in Reference [22] as 'frequency range of interest' and denoted as FROI. The second stage is to progressively increase the complexity of the system obtained in the first stage till the change of the eigenvalues within the prescribed radius is smaller than a given tolerance. Specifically, in the first stage CSEs are constructed with a iterative procedure. The iterative procedure starts with a model, called the baseline model, composed of a set of pre-selected components. Then, a set of candidate models are constructed, each with one more component than the baseline model. The spectrum, as well as the controllability and observability of each candidate model are calculated. All candidate models with uncontrollable or unobservable modes are eliminated from further search. In the remaining candidate models, the one with the smallest increase, with respect to the baseline model, in the spectrum radius is chosen as the new base line model. Then new candidate models are built upon the new baseline model and the procedure repeats till the spectrum of the baseline model in a certain iteration step reaches the specified radius. And the eigenvalues of the resultant model are CSEs. For the second stage, the procedure starts with the baseline model obtained in the last iteration of the first stage. Then a set of candidate models, each with one more component than the baseline model are constructed. The eigenvalues of each candidate model is calculated. Following that, the eigenvalues of each candidate model are compared to those of the baseline model. That is, the pair-wise distances of the eigenvalues of the candidate model and those of the base line model are obtained. For each candidate model, the maximum value of such pair-wise distances is defined as the change of CSE of the candidate model with respect to the baseline model. The candidate model with the largest change of CSEs is chosen as the new baseline model and the procedure repeats. The algorithm terminates when at certain iteration, the change of CSE is less than a prescribed tolerance.

CSE criterion has its advantages and disadvantages. On the advantage side, CSEs are important aspects of system dynamics and are very useful in system analysis and design. On the disadvantage side, CSE criterion has some foundamental restrictions and difficulties. In theory point of view, eigenvalues do not constitute a completed

description of an dynamic system. In fact, system zeros are equally important. In implementation point of view, a systematic and high efficient method is yet to be found for relating the system eigenvalues and system components. This explains the fact that variations of MODA, the only procedures that use CSE criterion up to now, have to conduct exhaustive searches in both of the two stages.

The MODA procedure is worthy of some discussions. The MODA procedure in Reference [22] has been successfully used for the analysis of an automobile suspension system. At the same time, this procedure has room for improvements. First, the resultant model may include the dynamics outside FROI, therefore the model may be unnecessarily complex. In fact during the second stage dynamics outside the FROI may be added to the model, for the sake of the convergence of the spectrum within the FROI. This is not be a good trade-off. Second, this procedure tries to simplify a model by removing certain physical components while keeping the parameters of the other components the same. As shown in Section 4.2, this imposes further restriction on model reduction.

As a conclusion, CSE criterion may become very useful given more understanding is achieved towards the profound relation between system eigenvalues and system components.

3.4 H_∞ Criterion

This section proposes a criterion based on the H_∞ norm of a certain error model. The physical meaning of the criterion is presented as well.

In areas such as control as well as system identification, the accuracy of a model's frequency response has for long time been a measurement for the model's goodness. The accuracy can be measured by the deviation of the frequency response of the model from that of the original system. Given the popularity of frequency-domain criteria in those areas, it is natural to consider using such a criterion for model order reduction.

This section proposes the H_∞ norm of an error model as a criterion. As shown in

this thesis, the use of H_∞ norm has the following advantages,

1. H_∞ norm takes into account the scenarios at all frequencies and all input directions,

2. No numerical simulation required,

3. Strict mathematical formulation and powerful mathematical tools can be developed for H_∞ norm related problems.

First, let us construct an error model that describes the difference between the original physical model and the reduced physical model, where the latter is obtained by removing some energy storage elements from the former. The error model is shown in Figure 3-9, where G and G_r are the transfer matrices of the original and the reduced systems respectively. Also, the input to the error model (which according to the structure of the error model is the input to the original and the reduced system), the output of the original system, the output of the reduced system and the output of the error model are denoted as u, y, y_r and e respectively. The error model, whose transfer matrix is denoted as G_{error}, compares the output y of the original system and the output y_r of the reduced system, and produces an error output. If the error output is small for all inputs with unit magnitudes, the reduced model is taken as a good simplification of the original one.

Second, let us consider the use of the H_∞ norm of this error model as the criterion for the accuracy of the reduced model. This choice is based on the time and frequency domain interpretation of the H_∞ norm. In the time domain, H_∞ norm of G_{error} can be written as [17],

$$\|G_{error0}(s)\|_\infty = \max_{\|u(t)\|_2=1} \|e(t)\|_2 \tag{3.8}$$

which is the largest 2-norm of the error for *all* inputs with unit 2-norm. In frequency domain, $\|G_{error}\|_\infty$ can be written as,

$$\|G_{error}(s)\|_\infty = \max_\omega \bar{\sigma}(G_{error}(j\omega)) \tag{3.9}$$

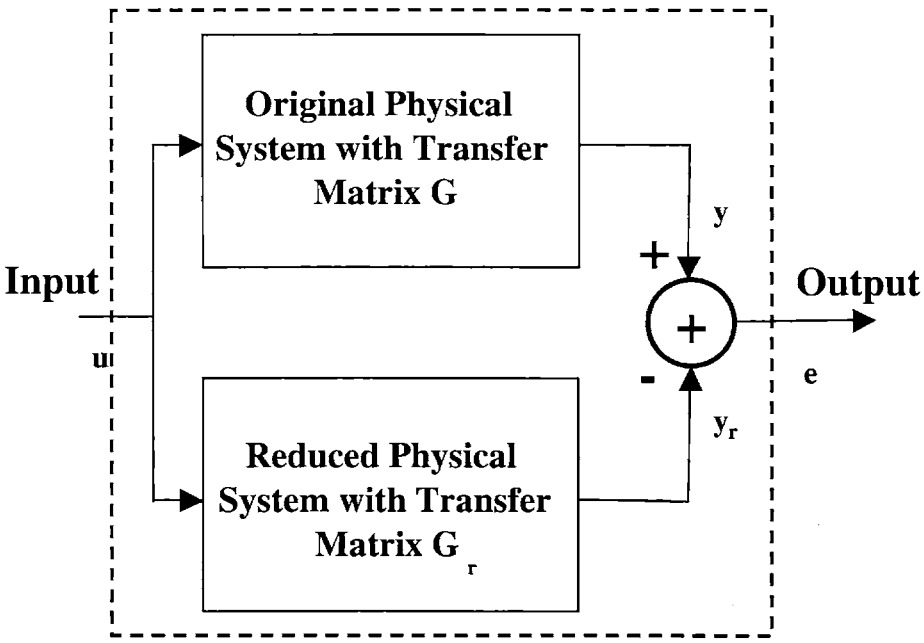

Figure 3-9: Error Model

which is the largest gain of G_{error} for all frequency points. Thus, if $\|G_{error}\|_\infty$ is small, the frequency response of the original model and that of the reduced model are close at *every* frequency point. Since the frequency response is a complete description of an LTI system, a reduced system is indeed a good approximation of the original system the H_∞ norm of the error model is small.

With the notations in Figure 3-10, the transfer matrix of the error model can be written as,

$$G_{error} = G - G_r \tag{3.10}$$

Accordingly, the error margin γ_p as in Figure 1-1 is chosen as the largest allowed H_∞ norm of the error model. In other words, a reduced system is acceptable if it satisfies,

$$\|G - G_r\|_\infty < \gamma_p \tag{3.11}$$

For a specific problem, the user has the freedom of choosing γ_p. This is because the error model and the algorithm for determining the reduced model as presented later in the thesis do not impose any requirement on the choosing of γ_p. For example, one can choose γ_p to be a small number, say 5 % or 3 % of the smallest gain in the frequency range of interest. Or one can choose γ_p to be a small number compared to the dc component of the frequency response. As always one shall be careful when choosing a specific error margin and understand the its meanings and implications.

In many applications, a system's dynamic behavior is of interest in certain frequency range only. In such cases, one can add input/output filters to the error model in Figure 3-9 to specify the dynamic properties of interest. The resultant model is shown in Figure 3-10. The detailed discussion on the error model with filters is in Section 4.4.

Finally, one shall be aware of the limitation of this error model. Essentially, H_∞ norm is a description of LTI systems and therefore this error model shall be used for LTI systems. This approach may be applied to nonlinear systems that can be sufficiently approximated with linearization, or time-variant systems that can be sufficiently approximated with piece-wise time invariant systems. This error model

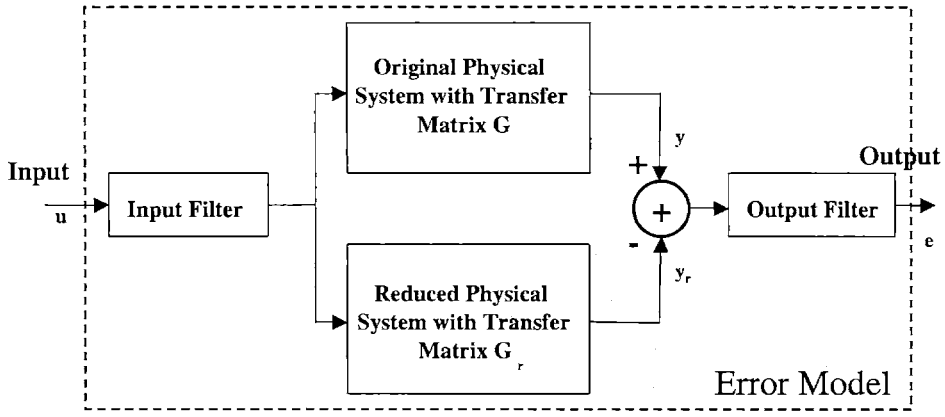

Figure 3-10: Error Model

shall not be used beyond its capacity.

3.5 Summary

This chapter focuses on the discussion of criteria for model reduction in physical domain. Existing criteria are evaluated, along with the algorithms that implement them. Furthermore, a criterion based on the H_∞ norm of some error model is presented. This criterion has some advantage over the existing ones.

Chapter 4

Mathematical Formulation of Model Reduction in the Physical Domain

4.1 Introduction

This chapter proposes the idea of formulation of the model reduction problem as an optimization problem. This idea has widened the scope of model reduction in the physical domain and led to simpler reduced models. Existing procedures for model reduction in the physical domain[18, 19, 21, 24] focus on the removal of some physical components while leaving the parameters of the others unchanged. However, it is well known that some physical components in a dynamic system may have a strong coupling with one another and thus make contributions to the dynamic behavior of the overall system as a whole. Therefore, some physical components can be removed only if the parameters of the other components are adjusted accordingly. Consequently, if the parameters of a system are allowed to change, more components may be removed. Existing procedures may not identify and eliminate such components. To solve this problem, this thesis formulates the model reduction problem as an optimization problem. This idea is based on the fact that in principle, one can test all

legitimate reduced models with all parameter combinations and choose the best one, which is the one with the minimum number of energy storage elements. Obviously, testing all possible reduced systems is not realistic. But with more sophisticated optimization techniques, one can expect to develop a search procedure that gives an answer in reasonable time. The transform from the model reduction problem to an optimization problem with BMI constraints is discussed in detail in this section. The solution of this optimization and the proof of convergence is presented the next chapter.

4.2 Expanding the Scope of Model Reduction

This section discusses the necessity of expanding the scope of model reduction in the physical domain. Specifically, one needs to consider changing all system parameters in the model reduction procedure. In the past, researchers have focused on removing some elements while keeping the parameters of others unchanged [18, 19, 21, 24]. This notion is a straight forward extension of everyday experience. However, it has brought about excessive restrictions on model reduction.

Due to the coupling within the system, a set of elements can make contribution to the system dynamics as a whole. Therefore, in model reduction, all parameters shall be considered simultaneously. For example, consider the system show in Figure 4-1. The component parameters are $M_1 = 10$, $M_2 = 1$, $k_1 = 1$, $k_2 = 1$, $R_1 = 1$, $R_2 = 1$ and $R_3 = 1$. The input and the output of the system are the velocity at the left end of the system and the displacement associated with k_1 respectively. With the generalized momenta associated with the masses and the generalized displacements associated with the springs as state variables, i. e. with the state vector $[p_1, p_2, q_1, q_2]$,

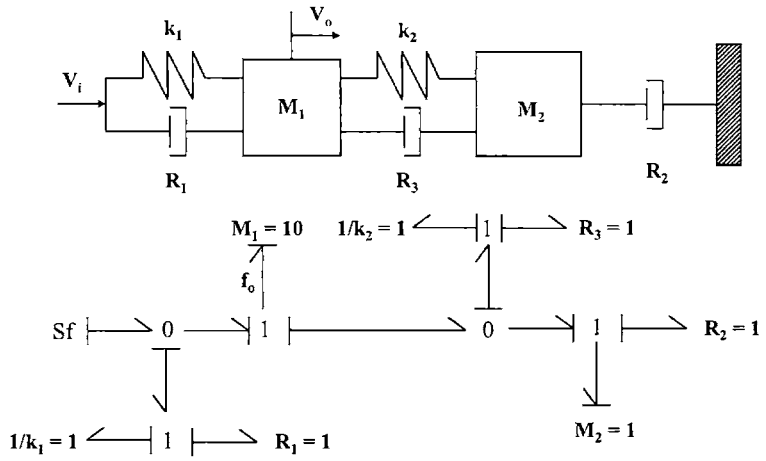

Figure 4-1: A Spring-Mass-Damper System

the state space matrices can be written as,

$$
\begin{aligned}
\mathbf{A} &= \begin{bmatrix} -\frac{(R_1+R_3)}{M_1} & \frac{R_3}{M_2} & -k_1, 0 & \\ \frac{R_3}{M_1} & -\frac{R_2+R_3}{M_2} & k_1 & -k_2 \\ \frac{1}{M_1} & -\frac{1}{M_2} & 0 & 0 \\ 0 & \frac{1}{M_2} & 0 & 0 \end{bmatrix} \\
\mathbf{B} &= \begin{bmatrix} 1 & 0 & 0 & 0 \end{bmatrix}^T \\
\mathbf{C} &= \begin{bmatrix} 0 & 0 & k_1 & 0 \end{bmatrix} \\
\mathbf{D} &= 0
\end{aligned} \tag{4.1}
$$

The frequency response of the system is shown in Figure 4-2 with solid lines. The pole-zero plot is shown in Figure 4-3 as well. From Figure 4-2, one can see that the bode plot of the system is quite similar to that of a second order system in its 3db band width which extends up to 0.3 rad/sec. At the same time, since there is a significant peak at the frequency of $0.2 rad/sec$, any reduced model shall be at least second order. Indeed, one can construct a second order system that approximates this fourth order system. In this reduced system, as shown in Figure 4-4, C_2 and I_2 are set to be zero. Furthermore, in the reduced model, the parameters of $k = 0.6667$

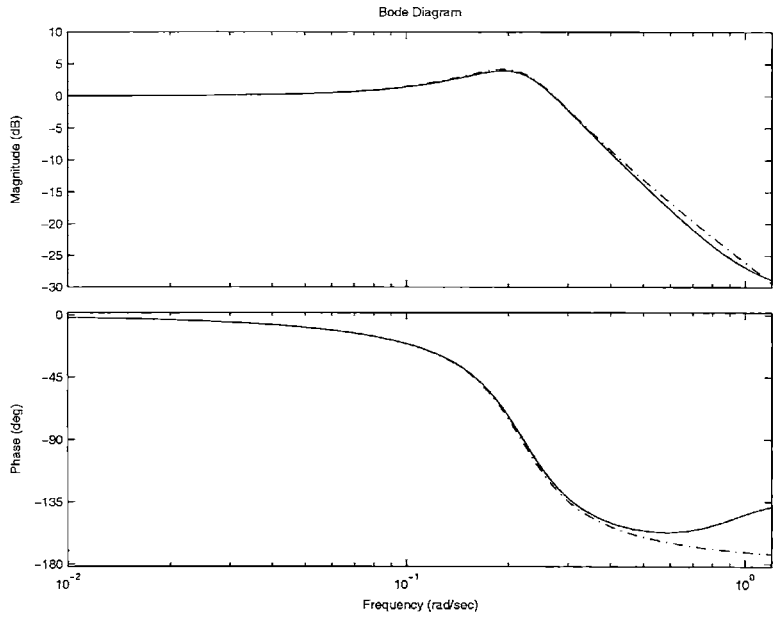

Figure 4-2: Frequency Response of the Spring-Mass-Damper System

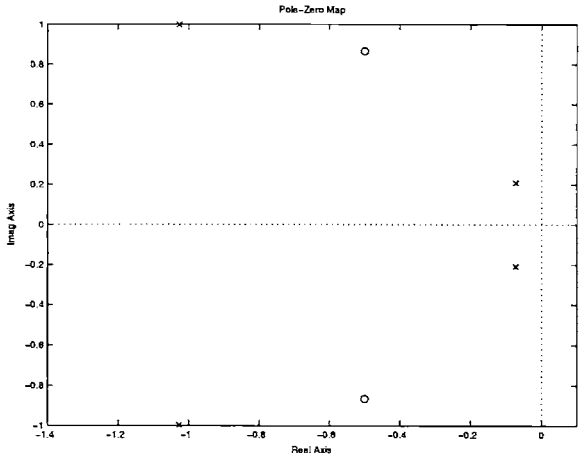

Figure 4-3: Pole-Zero Plot of the Spring-Mass-Damper System

and $I = 14$ are quite different from those of $k_1 = 1$ and $I_1 = 10$ in the original model. The frequency response of the reduced system is shown in Figure 4-2 with dashed lines, which indicate that the reduced model is a good simplification. The H_∞ norm of the corresponding error model is 0.07. Since the system is an SISO system, the H_∞ norm of the error model is the maximum value of the magnitude of the transfer function of the error model. Compare to the magnitude of the frequency response of the original system, which is greater than 0.5 in the 3db band width, the error is indeed very small. On the other hand, if the parameters of the components of the reduced system must be equal to those of the original system, in other words if I of the reduced model must equal to I_1 and same for C, one would have greater error. In this case, the H_∞ norm of the error model is 1.4, twenty times of the reduced model in Figure 4-4. The frequency responses of the original model and the model with I and C fixed is shown in Figure 4-5[1].

As a conclusion, the scope of model reduction shall be expanded to include proper adjustment of system parameters for better results.

4.3 Formulation of Model Reduction Problem as Optimization Problem

4.3.1 Model Reduction in an Optimization Perspective

This section formulates the model reduction problem as a optimization problem. As mentioned in the introduction of this chapter, one could search all parameter[2] combinations to find a system that satisfies Equation (3.11) and has the maximum

[1] One may ask why the mass in the reduced model is not the sum of the masses in the original system $M_1 + M_2 = 11$. In fact, in the original system the connection between the two masses $k_2 = 1$ is far from rigid. Therefore in most frequency ranges within the band width M_1 and M_2 do not move at the same velocity as a rigid body. So no wonder in the reduced model the mass is not the sum of M_1 and M_2. In fact, if one construct a second order system with the structure of the reduced model and set the spring coefficient to be 1 and the mass to be 11, one would have the H_∞ norm of the error model be 1.36, which is far larger than the error of the reduced model introduced above.

[2] From this point on, the word 'parameter' refers to the parameters of energy storage elements, i.e. I and C, of a system unless otherwise stated.

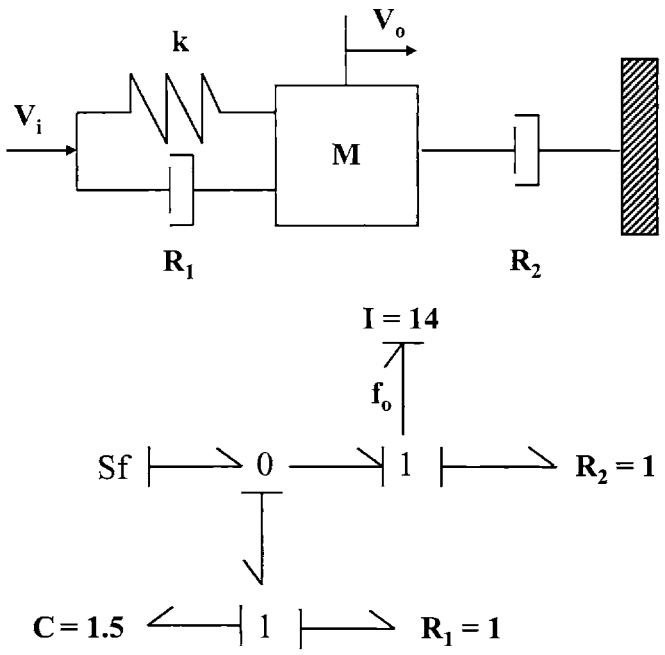

Figure 4-4: Reduced Spring-Mass-Damper System

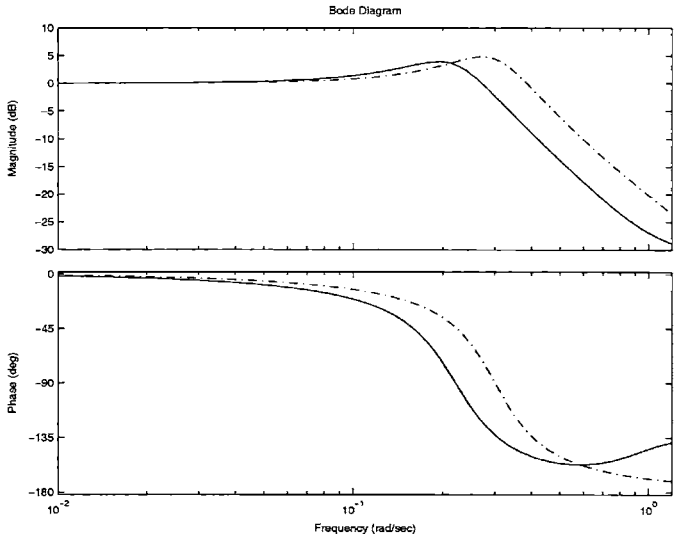

Figure 4-5: Frequency Response: Solid: Original Model, Dashed: Reduced Model with I = I_1 and $C = C_1$

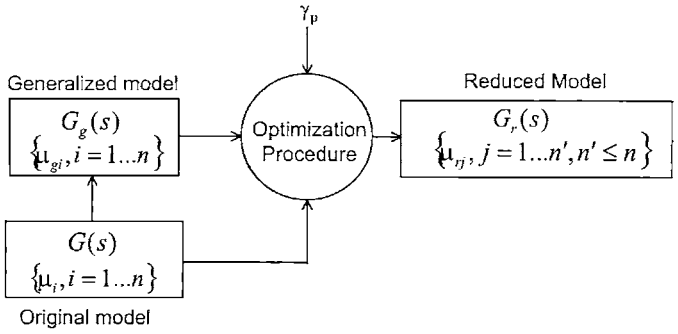

Figure 4-6: Outline of the Optimization Procedure

number of I's and C's set to zero. However, it is impractical to literally try out all possible parameter combinations because there are infinitely many of them. To search the parameter space efficiently and find the best result, one needs the help of sophisticated optimization tools.

Figure 4-6 illustrates the proposed optimization procedure for model reduction. The original model SYS_o is an n^{th} order system with a transfer matrix G. The parameters are denoted as μ_i. The generalized model SYS_g is a system that has the same structure with the original model while its parameters, μ_{gi}, can be chosen from all positive real numbers. The transfer matrix of the generalized model is denoted as G_g. The optimization procedure to be developed searches over the set of all generalized models and produces a reduced model with as many parameters as possible set to zero and satisfies Equation (3.11).

An optimization problem has the following two essential aspects,

- Index function

- Constraints

which are discussed in the following sections.

4.3.2 Choosing an Index Function

In this section, an index function for the optimization problem associated with model reduction is constructed. The goal of model reduction is to remove as many physical components as possible. So the index function shall be constructed in such a way that the function reaches optimum when as many components as possible are removed. This problem is solved in two steps,

1. Prove that an energy storage element can be removed if its parameter can be set to a sufficiently small positive number,

2. Find an index function that reaches maximum when as many parameters as possible are set to be sufficiently small.

Denote transfer matrices of the system with μ_{gi} set to zero (and the same parameters with the original system otherwise) as $G_{\mu_{gi}=0}$. Denote the system with μ_{gi} as a variable as $G_{\mu_{gi}}$ and the system with μ_{gi} has a positive value δ as $G_{\mu_{gi}=\delta}$. With these notations we have,

Theorem 1 *If for a sufficiently small $\delta > 0$, $\|G - G_{\mu_{gi}=\delta}\|_\infty < \gamma_p$ and if $G_{\mu_{gi}=0}$ is stable, then $\|G - G_{\mu_{gi}=0}\|_\infty < \gamma_p$ holds.*

Theorem 1 basically says that if the parameter of a component can be set to be sufficiently small, the component can be removed[3]. To prove Theorem 1, some existing results, listed below, are used.

Lemma 1 *For an n^{th} order causal LTI system, when the state vector $\mathbf{x}$ is composed of the flows associated with inductances and efforts associated with capacitances, the state space equation can be written as [36],*

$$\begin{bmatrix} \mu_{g1} & & \\ & \ddots & \\ & & \mu_{gn} \end{bmatrix} \frac{d}{dt}\mathbf{x} = \mathbf{A}_p\mathbf{x} + \mathbf{B}_p\mathbf{u}$$
$$\mathbf{y} = \mathbf{C}_p x + \mathbf{D}_p\mathbf{u} \tag{4.2}$$

[3] $G_{\mu_{gi}=0}$ is stable means when a energy storage element is removed from the original system, the reduced system is stable.

where $\mathbf{A}_p, \mathbf{B}_p, \mathbf{C}_p$ *and* $\mathbf{D}_p$ *are constant matrices.*

Lemma 2 *If* $\varphi_1(x_1, \ldots, x_n), \ldots, \varphi_m(x_1, \ldots, x_n)$ *are continuous functions of* $x_1, \ldots, x_n$ *and* $f(y_1, \ldots, y_m)$ *is a continuous function of* $y_1, \ldots, y_m$*, then*

$$u = f(\varphi_1(x_1, \ldots, x_n), \ldots, \varphi_m(x_1, \ldots, x_n)) \tag{4.3}$$

is a continuous function of $x_1, \ldots, x_n$*[37].*

Lemma 3 *If* $f(\mathbf{x})$ *and* $g(\mathbf{x})$ *are continuous with respect to* $\mathbf{x}$*, then* $\frac{f(\mathbf{x})}{g(\mathbf{x})}$ *is continuous with respect to* $\mathbf{x}$ *except for the points where* $g(\mathbf{x}) = 0$ *[37].*

Proof of Theorem 1

First, let us prove that $\|G_{\mu_{gi}=0} - G_{\mu_{gi}}\|_\infty$ is a continuous function of μ_{gi} in the neighborhood of $\mu_{gi} = 0$. Since the H_∞ norm is the largest singular value of the transfer matrix along the $j\omega$ axis, only the value of the transfer matrix along the imaginary axis is relevant. According to Lemma 1, $G_{\mu_{gi}}$ evaluated along $j\omega$ axis can be written as,

$$\begin{aligned} G_{\mu_{gi}}(j\omega) &= \mathbf{C}_p(j\omega \begin{bmatrix} \mu_{g1} & & \\ & \ddots & \\ & & \mu_{gn} \end{bmatrix} - \mathbf{A}_p)^{-1}\mathbf{B}_p + \mathbf{D}_p \\ &= \mathbf{C}_p \frac{adj\left(j\omega \begin{bmatrix} \mu_{g1} & & \\ & \ddots & \\ & & \mu_{gn} \end{bmatrix} - \mathbf{A}_p\right)}{det\left(j\omega \begin{bmatrix} \mu_{g1} & & \\ & \ddots & \\ & & \mu_{gn} \end{bmatrix} - \mathbf{A}_p\right)}\mathbf{B}_p + \mathbf{D}_p \end{aligned} \tag{4.4}$$

According to the definition of determinant,

$$det\left(j\omega\begin{bmatrix}\mu_{g1} & & \\ & \ddots & \\ & & \mu_{gn}\end{bmatrix}-\mathbf{A}_p\right) \tag{4.5}$$

as well as the terms in,

$$adj\left(j\omega\begin{bmatrix}\mu_{g1} & & \\ & \ddots & \\ & & \mu_{gn}\end{bmatrix}-\mathbf{A}_p\right) \tag{4.6}$$

are polynomials of μ_{gi}, which are continuous of μ_{gi}. Since $G_{\mu_{gi}=0}$ is stable, every entry of $G_{\mu_{gi}=0}$ must be finite on $j\omega$. Therefore (4.5) evaluated at $\mu_{gi}=0$ is nonzero on $j\omega$. It has already been shown that (4.5) is continuous with respect to μ_{gi}, therefore there exist a neighborhood of $\mu_{gi}=0$ in which (4.5) is nonzero. Therefore according to Lemma 3 every entry of $G_{\mu_{gi}}$ is continuous in this neighborhood. Now the entries of $G_{\mu_{gi}=0}(j\omega)$ are independent of μ_{gi}, and the H_∞ norm of a matrix is a continuous function of the entries of the matrix. Thus according to Lemma 2, $\|G_{\mu_{gi}=0}-G_{\mu_{gi}}\|_\infty$ is a continuous function of μ_{gi}. Given $\|G_{\mu_{gi}=0}-G_{\mu_{gi}}\|_\infty|_{\mu_{gi}=0}=0$, we have $\forall\epsilon>0$, $\exists\delta$ such that $\forall\mu_{gi}<\delta$, $\|G_{\mu_{gi}=0}-G_{\mu_{gi}}\|_\infty<\epsilon$.

Given that $\|G-G_{\mu_{gi}=\delta}\|_\infty<\gamma_p$, $\exists\epsilon>0$ such that

$$\|G-G_{\mu_{gi}=\delta}\|_\infty+\epsilon<\gamma_p \tag{4.7}$$

due to continuity. On the other hand for a sufficiently small δ, we have,

$$\begin{aligned}
& \|G-G_{\mu_{gi}=0}\|_\infty \\
= \; & \|G-G_{\mu_{gi}=\delta}+G_{\mu_{gi}=\delta}-G_{\mu_{gi}=0}\|_\infty \\
\leq \; & \|G-G_{\mu_{gi}=\delta}\|_\infty+\|G_{\mu_{gi}=\delta}-G_{\mu_{gi}=0}\|_\infty \\
\leq \; & \|G-G_{\mu_{gi}=\delta}\|_\infty+\epsilon
\end{aligned}$$

$$< \gamma_p \tag{4.8}$$

End of Proof

Theorem 1 says a component can be removed if its parameter is sufficiently small, which is equivalent to say that it can be removed if the inverse of its parameter is sufficiently large. So in order to get the inverse of as many parameters as possible to be large, the author proposes the following index function,

$$\max L = \sum_{i=1}^{n} \frac{1}{\mu_{gi}} \tag{4.9}$$

Subject to,

$$\frac{1}{\mu_{gi}} \leq H \tag{4.10}$$

$$\|G - G_g\|_\infty < \gamma_p \tag{4.11}$$

where H is a sufficiently large number. The choice of H is discussed later in the section. Figure 4-7 is a plot of $L = \frac{1}{x_1} + \frac{1}{x_2}$ for the range of $x_1, x_2 \in [0.01, 2]$. From the figure one can see that L increases rapidly when either x_1 or x_2 is small, and increases more rapidly when both variables are small.

Before proceeding several symbols are introduced for future convenience. For the sake of succinctness from this point on $\frac{1}{\mu_{gi}}$ is denoted as μ_i'. Also, since L is continuous from now on only strict inequality signs are used in the constraints. Strictly speaking, now the goal is to find μ_{gi} such that the corresponding L is sufficiently close to its supreme. But to avoid unnecessary inconvenience the symbol of max is still used. Thus the optimization problem is now,

$$\max L = \sum_{i=1}^{n} \mu_i' \tag{4.12}$$

subject to,

$$\mu_i' < H \tag{4.13}$$

$$\|G - G_g\|_\infty < \gamma_p \tag{4.14}$$

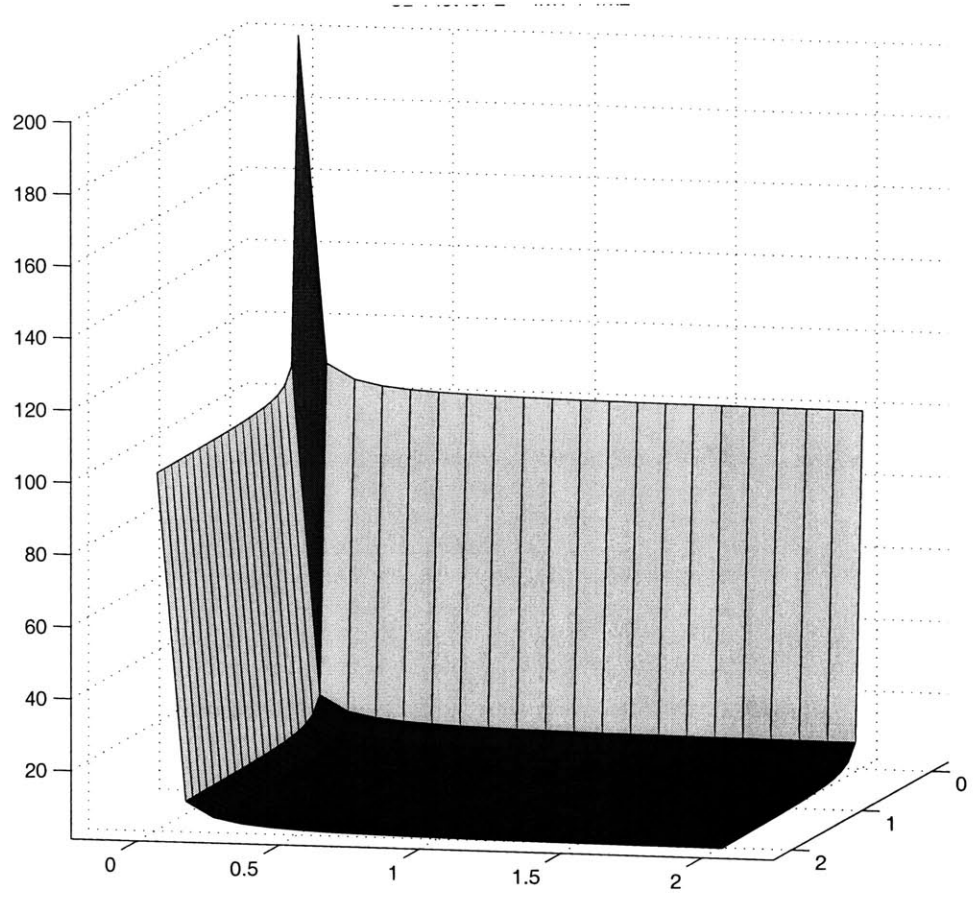

Figure 4-7: Plot of the Index Function $L = \frac{1}{x_1} + \frac{1}{x_2}$

Now it is a good time to discuss one of the constraints on the scope of this thesis, which is the systems under investigation are those whose frequency response is not very sensitive to energy storage elements with sufficiently small parameters. With this constraint, the solution of the proposed optimization problem corresponds to the parameter configuration where all removable components are squeezed to be sufficiently small, as made clear in later paragraphs. Strictly, the constraint can be written as following. Denote the parameters of the independent energy storage elements of the system as $\mu_i, \ldots, \mu_n$, and denote the corresponding transfer matrix of the system with these parameters be $\mathbf{G}(\mu_1, \ldots, \mu_n)$. The above-mentioned constraint can be represented as, $\forall \epsilon > 0$, $\exists \Delta_i$, such that $\forall \Delta_{1i}, \Delta_{2i} < \Delta$, $\|\mathbf{G}(\mu_1, \ldots, \mu_n)|_{\mu_i=\Delta_1} - \mathbf{G}(\mu_1, \ldots, \mu_n)|_{\mu_i=\Delta_2}\|_\infty < \epsilon$, $\forall i$ for all combinations of $\mu_j, j \neq i$. The physical meaning of the Δ_i is a threshold, and if the parameter of component i is less than the threshold, the dynamic behavior is no longer sensitive to the component. Physically, this constraint does not severely shrink the extent of the proposed procedure. In fact, the frequency response of a reasonably designed system shall not be sensitive to extremely small system parameters, which usually are parasitic parameters not considered in the design and not controllable in the manufacturing procedure.

Theoretically, H shall be chosen to be sufficiently large. H is sufficiently large if it satisfies two conditions,

1. An energy storage element can be removed if the corresponding μ_i' is sufficiently close to H.

2. The system frequency response is insensitive an energy storage component if its parameter is sufficiently close to H.

To search for a sufficiently large H, one can choose an initial value and follow the procedure in Figure 4-8, where η is a scaling factor greater than one. The initial value of H can be chosen several order of magnitudes greater than the inverse of the smallest system parameter.

For a specific industrial application, one can in fact choose H empirically. In engineering practice, an engineer usually knows before hand the smallest parameter

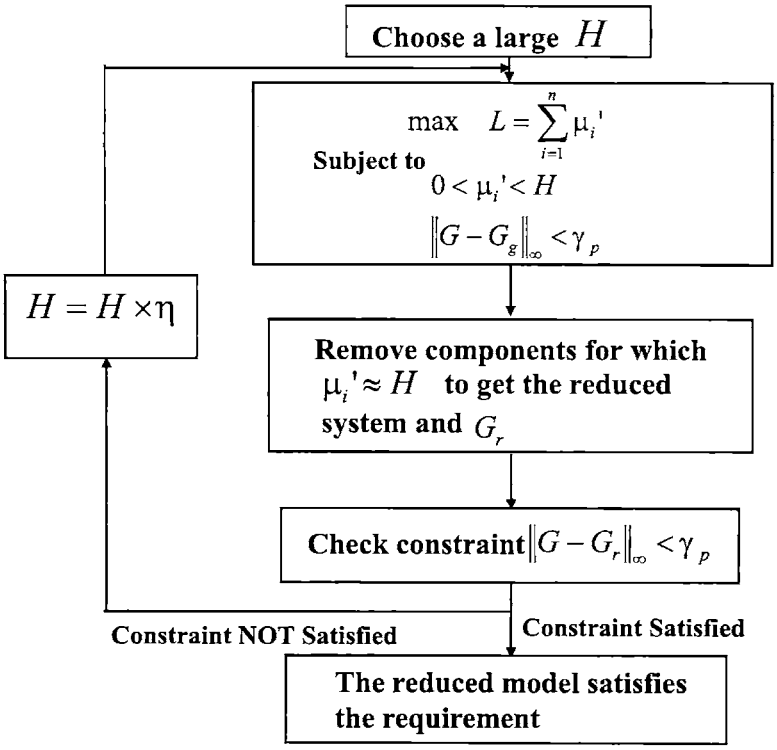

Figure 4-8: Progressive Procedure for Choosing H

that is possibly relevant in the system design and analysis. It is quite often sufficient to choose H to be several order of magnitude greater than the inverse the parameter[4].

The solution of the proposed optimization problem pushes the μ_i' of all removable components to be sufficiently close to H[5]. In fact, one question raised about the optimization procedure is that if the μ' corresponding to one particular component could increase in the vicinity of H in such a way that the parameters of other components that would get close to H are kept small. With the newly added constraint, this specific concern disappears, as illustrated in the following. Set the inverse of the parameter of one component, denoted as μ_1' without loss of generality, to be a value h_1 close to H [6] while satisfying the H_∞ norm of the error model, $\|\mathbf{G} - \mathbf{G}(\mu_1' = h_1)\|_\infty < \gamma_p$. Also, suppose the inverse of the parameter of another component, denoted as μ_2', can be set to h_2 sufficiently close to H given $\mu_1' = h_1$, i.e. $\|\mathbf{G} - \mathbf{G}(\mu_1' = h_1, \mu_2' = h_2)\|_\infty < \gamma_p$. In this case, the increase of μ_1' does not interfere with the increase of μ_2'. Actually, according to the newly added constrain on systems, if μ_1' increases to h_1', according to the newly added constraint on systems we have $\|\mathbf{G} - \mathbf{G}(\mu_1' = h_1', \mu_2' = h_2)\|_\infty < \gamma_p$ when ϵ is sufficiently small, e.g. several order of magnitude smaller than the tolerance of the optimization problem. In other words, μ_2' can increase independent of μ_1'.

One interesting implication of this index function lies in causality perspective. In the process of searching the elements that can be removed, no element is actually removed and therefore there is no need to reassign causality and recalculate the system equations. This could save significant time for the search of a reduced model.

---

[4]Also, one can choose different upper boundaries for μ_i', denoted as H_i', instead of using a single H, as long as all H_i' satisfies the above listed two conditions. A set of well chosen H_i' may facilitate the search for the optimum. On the other hand, there may or may not be strict rules for the choice of a set of 'good' H_i', since the optimization problem to be solved, i.e. BMI, is known to be complex. So if one would like to take advantage of various H_i' rather than a single H, it is his/her own responsibility to make sure the choice contributes to the optimization search positively.

[5]If some physical component(s) is removable, then the optimum point is sufficiently close to the boundary of the area under search. If no physical component is removable, the optimum point does not always occur at the boundary. Because in this case, the optimum would occur where μ_i' significantly less than H for all i.

[6]As mentioned before, H shall be chosen to satisfy the above mentioned two conditions.

4.3.3 Relating System Parameters and H_∞ Norm

One more issue left is that the constraint (4.14) does not contain the decision variables μ_i' explicitly. This problem is solved in two steps,

1. Obtain system state space equations that explicitly contain μ_i',

2. Represent the H_∞ norm of the error model with system state space equations.

A parameterization of causal LTI systems with respect to μ_i' can be found in Reference [38]. Specifically, when the generalized momenta associated with inductances and the generalized displacements associated with capacitances are chosen as state variables, the state space equations of the generalized model can be written as,

$$\mathbf{A}_g = \mathbf{J}_A\mathbf{E}_g \quad \mathbf{B} \quad \mathbf{C}_g = \mathbf{J}_C\mathbf{E}_g \quad \mathbf{D} \tag{4.15}$$

where,

$$\mathbf{E}_g = \begin{bmatrix} \mu_1' & & \\ & \ddots & \\ & & \mu_n' \end{bmatrix} \tag{4.16}$$

and $\mathbf{J}_A, \mathbf{B}, \mathbf{J}_C, \mathbf{D}$ are independent of μ_i'.

The H_∞ norm and the system state space equation can be related via positive definite lemma [33],

Lemma 4 (Positive Definite Lemma) *Let $\gamma > 0$, let $\mathbf{A}$, $\mathbf{B}$, $\mathbf{C}$ and $\mathbf{D}$ be a state space realizetion of a stable system $\mathbf{G}(s)$, then the following conditions are equivalent,*

1. $\|G\|_\infty < \gamma$

2. *There exist $\mathbf{P} > 0$ such that,*

$$\begin{bmatrix} \mathbf{PA} + \mathbf{A}^*\mathbf{P} & \mathbf{PB} & \mathbf{C}^* \\ \mathbf{B}^*\mathbf{P} & -\gamma\mathbf{I} & \mathbf{D}^* \\ \mathbf{C} & \mathbf{D} & -\gamma\mathbf{I} \end{bmatrix} < 0 \tag{4.17}$$

Let the state A state space realization for $G - G_g$ is [34],

$$\begin{bmatrix} \mathbf{A} & \mathbf{0} \\ \mathbf{0} & \mathbf{A}_g \end{bmatrix} \quad \begin{bmatrix} \mathbf{B} \\ \mathbf{B} \end{bmatrix} \quad \begin{bmatrix} \mathbf{C} & -\mathbf{C}_g \end{bmatrix} \quad \mathbf{D} - \mathbf{D} = \mathbf{0} \tag{4.18}$$

Combining (4.15) and (4.18) gets the state space realization of $\mathbf{G} - \mathbf{G}_g$ that explicitly contains μ_i',

$$\begin{bmatrix} \mathbf{A} & \mathbf{0} \\ \mathbf{0} & \mathbf{J}_A \end{bmatrix} \begin{bmatrix} \mathbf{I} & 0 \\ 0 & \mathbf{E}_g \end{bmatrix} \quad \begin{bmatrix} \mathbf{B} \\ \mathbf{B} \end{bmatrix} \\ \begin{bmatrix} \mathbf{C} & -\mathbf{J}_C \end{bmatrix} \begin{bmatrix} \mathbf{I} & 0 \\ 0 & \mathbf{E}_g \end{bmatrix} \quad \mathbf{D} - \mathbf{D} = \mathbf{0} \tag{4.19}$$

Substitute (4.19) into (4.17) leads to the following result,

Theorem 2 *The constraint of* $\|G - G_p\|_\infty < \gamma_p$ *is equivalent to* $\exists$ *symmetric* $\mathbf{P} > 0$,

$$\begin{bmatrix} \begin{bmatrix} \mathbf{I} & 0 \\ 0 & \mathbf{E_g} \end{bmatrix} \begin{bmatrix} \mathbf{A^T} & 0 \\ 0 & \mathbf{J_A^T} \end{bmatrix} \mathbf{P} + \mathbf{P} \begin{bmatrix} \mathbf{A} & 0 \\ 0 & \mathbf{J_A} \end{bmatrix} \begin{bmatrix} \mathbf{I} & 0 \\ 0 & \mathbf{E_g} \end{bmatrix} & \mathbf{P} \begin{bmatrix} \mathbf{B} \\ \mathbf{B} \end{bmatrix} & \begin{bmatrix} \mathbf{I} & 0 \\ 0 & \mathbf{E_g} \end{bmatrix} \begin{bmatrix} \mathbf{C^T} \\ -\mathbf{J_C^T} \end{bmatrix} \\ \begin{bmatrix} \mathbf{B^T} & \mathbf{B^T} \end{bmatrix} \mathbf{P} & -\gamma_P \mathbf{I} & \mathbf{0} \\ \begin{bmatrix} \mathbf{C} & -\mathbf{J_C} \end{bmatrix} \begin{bmatrix} \mathbf{I} & 0 \\ 0 & \mathbf{E_g} \end{bmatrix} & \mathbf{0} & -\gamma_P \mathbf{I} \end{bmatrix} < 0 \tag{4.20}$$

Constraint (4.20) contains μ_i' explicitly. For the sake of compactness from now on denote the left hand side of Inequality (4.20) as $\mathbf{M}(\mu_i', \mathbf{P})$.

Constraint (4.20) is obviously a bilinear matrix inequality (BMI) constraint since the constraints contain multiplication of decision variables μ_i' and components of $\mathbf{P}$.

In summary, the model reduction problem can be formulated as the optimization problem as below,

$$\max L = \sum_{i=1}^{n} \mu_i' \tag{4.21}$$

subject to,

$$0 < \mu_i' < H \ \forall i \tag{4.22}$$

$$\mathbf{P} > 0 \tag{4.23}$$

$$\mathbf{M}(\mu_i', \mathbf{P}) < 0 \tag{4.24}$$

where n μ_i' and $n' = n(2n+1)$ independent components of the symmetric matrix $\mathbf{P}$ are decision variables.

4.4 Error Model with Input/Output Filters

The interpretation of H_∞ norm as in Equation (3.9) leads to the idea of using filters to specify the frequency range of interest for model reduction. In many applications, the system dynamic behavior is of interest only within a limited frequency range. In such cases, the reduced model is required to have a similar frequency response to the original model within the given range. To produce such reduced models, one can use input/output filters with the passing bands set to be the interested frequency ranges only, and therefore exclude the frequency components of the error output outside the interested frequency range. The error model with input/output filters is shown in Figure 3-10.

The use of filters is illustrated in the following example. In Figure 4-9, the solid lines and the dashed lines are the frequency responses of a fourth order and a second order system respectively. If the frequency range of interest is $\omega \leq 1 rad/sec$, then the second order system is a good simplification of the fourth order system. However, the two systems differs significantly in the frequency range near $\omega = 4 rad/sec$. In fact, the magnitude of the frequency response of the error model without filter is shown in the left half of Figure 4-10. Since the system under consideration is an SISO system (and therefore so is the error model), the H_∞ norm of the error model is the maximum of the magnitude of the frequency response of the error model. Then one can read from the figure that the H_∞ norm of the error model is more than 0.9. But this data is actually irrelevant because such large error happens outside the frequency range of interest. The right half of the Figure 4-10 shows the magnitude of an error model with an output filter. The filter is a tenth order Butterworth filter with cut off frequency at $1 rad/sec$, heavily attenuating the frequency components outside the range of interest. Now the H_∞ norm of the error model is approximately 0.014. The

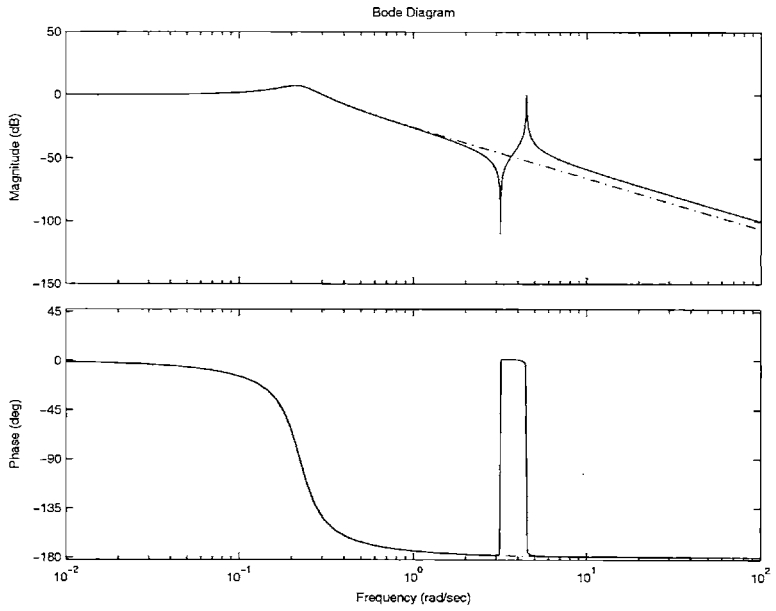

Figure 4-9: Bode Plot of a Fourth Order and a Second Order System

error is much smaller than the magnitude of the frequency response of the original system in its band width in the interested frequency range, which is in the order of magnitude of 1. This result is consistent with our inspection of the bode plots, i.e. the second order system is a good approximation of the fourth order system.

As shown in Figure 3-10, the error model is a series connection of the input filter, the system in Figure 3-9 and the output filter. Let a state space realization of the input filter[7] be $\mathbf{A}_{in}$, $\mathbf{B}_{in}$, $\mathbf{C}_{in}$ and $\mathbf{D}_{in}$, and that of the output filter be $\mathbf{A}_{out}$, $\mathbf{B}_{out}$, $\mathbf{C}_{out}$ and $\mathbf{D}_{out}$. Also let the corresponding state vector be $\mathbf{x}_{in}$ and $\mathbf{x}_{out}$ respectively. Furthermore, a state space realization of the system in Figure 3-9 is provided in (4.18). Then with some trivial and tedious algebraic manipulation[8] a state space realization

[7]Since for input/output filters only their transfer matrices are relevant, any state space realization can be used.

[8]See Appendix C.

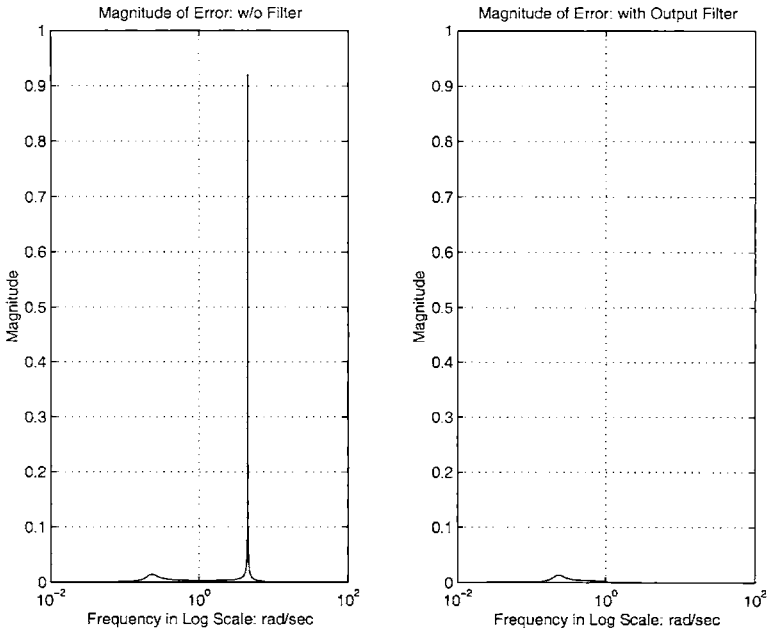

Figure 4-10: Magnitudes of the Outputs of Error Models

of the overall error model can be obtained as,

$$
\begin{aligned}
A_{error} &= \begin{bmatrix} \mathbf{A}_{in} & 0 & 0 \\ 0 & \mathbf{A}_{out} & \mathbf{B}_{out}\begin{bmatrix} \mathbf{C} & -\mathbf{J}_C \end{bmatrix} \\ \begin{bmatrix} \mathbf{B} \\ \mathbf{B} \end{bmatrix}\mathbf{C}_{in} & 0 & \begin{bmatrix} \mathbf{A} & 0 \\ 0 & \mathbf{J}_A \end{bmatrix} \end{bmatrix} \begin{bmatrix} \mathbf{I} & 0 & 0 \\ 0 & \mathbf{I} & 0 \\ 0 & 0 & \begin{bmatrix} \mathbf{I} & 0 \\ 0 & \mathbf{E}_g \end{bmatrix} \end{bmatrix} \\
\mathbf{B}_{error} &= \begin{bmatrix} \mathbf{B}_{in} \\ 0 \\ \begin{bmatrix} \mathbf{B} \\ \mathbf{B} \end{bmatrix}\mathbf{D}_{in} \end{bmatrix} \\
\mathbf{C}_{error} &= \begin{bmatrix} 0 & \mathbf{C}_{out} & \mathbf{D}_{out}\begin{bmatrix} \mathbf{C} & -\mathbf{J}_C \end{bmatrix} \end{bmatrix} \begin{bmatrix} \mathbf{I} & 0 & 0 \\ 0 & \mathbf{I} & 0 \\ 0 & 0 & \begin{bmatrix} \mathbf{I} & 0 \\ 0 & \mathbf{E}_g \end{bmatrix} \end{bmatrix} \\
\mathbf{D}_{error} &= 0
\end{aligned}
\tag{4.25}
$$

where Is' are unit matrices with appropriate dimensions.

Equation (4.25) is the same as (4.19) except for some constant terms. One can substitute (4.25) into (4.17) and get a BMI constrain of the same form. Therefore any future result developed for the case without filters applies directly to the case with filters.

Besides providing a means for delineating the frequency range of interest, the input/output filters can be used in many creative ways to expand or enhance the proposed model reduction procedure. One good example is the use of the output filter in the case where the output of the original system is small and the phase error must be confined. In this case, an output filter can be designed if the following quantities are known in advance,

1. The relevant frequency range,

2. The order of the magnitude of the output of the original system in the relevant frequency range.

This may well be the case in many engineering applications. One can use an output filter that magnifies the error output in the relevant frequency range. It is already known that, when the magnitude of the output of the original system is large enough, a constraint on H_∞ norm of the error model requires the phase of the original model and the reduced model to be sufficiently close. Therefore, if the amplification of the filter is designed such that during the relevant frequency range, the magnitude of the output of the original system multiply by the amplification shall be large enough, the phases of the original and the reduced models are required to be sufficiently small by the H_∞ norm constraint. Another example may include the use of the filters to specify the input/output directions of special interest, in which the case the input/output filters shall be designed to have large amplification at these directions.

4.5 Summary

This chapter focuses on the formulation of model reduction problem as an optimization problem. Efforts have been made to expand the scope of model reduction in physical domain as well as give it a rigorous mathematical frame. Furthermore, no causality change occurs during the search process, which may save significant time rebuilding system equations.

Chapter 5

Solving the BMI Problem Associated with Model Reduction

5.1 Introduction

Optimization problems with BMI constraints have raised great interest in system and control area in the last few years. Many problems in the area can be reduced to BMI form in an elegant manner. At the same time, it is widely known that BMI problems are difficult problems.

Significant efforts have been invested in developing procedures to find global optimum of BMI problems [39, 40, 41, 42, 43, 44, 45, 47, 48], most of which based on variations of the branch-and-bound method. Although in most cases the convergence of the algorithms to the global optimum is proved, in practice branch-and-bound procedures are well known for their low efficiency.

In this chapter, a branch-and-bound procedure based on the partitioning of part of the decision variable space is presented. With the partitioning of part of the decision variable space one can expect to reduce the computational cost of solving the problem and achieve better efficiency. The convergence of the algorithm to the global optimum is proved. In the numerical experiments the algorithm exhibits acceptable convergence rate.

In Section 5.2, the branch-and-bound (denoted as BB hereafter) method is briefly

reviewed. A algorithm for model reduction based on BB is presented in Section 5.3. Section 5.4 proves the convergence of the algorithm. The last section of summarizes this chapter.

5.2 Review of Branch-and-Bound Procedure

The BB method is mostly used for solving difficult optimization problems. This section gives a very brief review of the method. A detailed presentation of the method can be found in Reference [49]. An application oriented introduction can be found in [50].

The following is a general outline of the BB method for finding the ϵ-optimum of function f over a set $\mathcal{D}$ [49],

1. Start with a relaxed set $T_0 \supseteq \mathcal{D}$ and partition T_0 into finitely many subregions T_i, $i \in Z^+$.

2. For each subregion T_i, find $\beta(T_i)$ and $\alpha(T_i)$ that,

$$\beta(T_i) \leq sup f(T_i \cap \mathcal{D}) \leq \alpha(T_i) \tag{5.1}$$

   In other words, $\beta(T_i)$ and $\alpha(T_i)$ are the lower and upper bounds of the maximum value of f on $\mathcal{D}$. Then choose $\lambda = \max_i \beta(T_i)$, $\zeta = \max_i \alpha(T_i)$ satisfy,

$$\lambda \leq \max f(\mathcal{D}) \leq \zeta \tag{5.2}$$

   Thus λ and ζ are the lower and upper bounds of the overall optimum.

3. If $\zeta - \lambda < \epsilon$ then stop,

4. Otherwise remove subregions T_i for which $\alpha(T_i) \leq \lambda + \epsilon$, further partition the remaining subregions and go to 2.

Figure 5-1 is an illustration of the procedure. In the first step the region under search is divided into four subregions. In the second step the upper and lower bounds

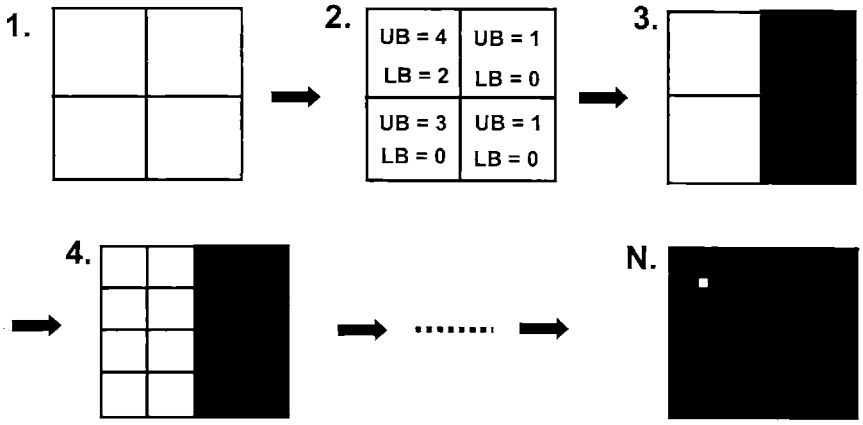

Figure 5-1: Illustration of the BB Method

of the optimum for each subregion are calculated. Apparently the maximum will not occur in the two subregions on the right because the upper bounds for of the maximum over these two regions are smaller than the lower bounds of the maximum of the upper left region. Therefore the two regions on the right are eliminated from the future search. The remaining regions are further divided in Step 4, and the algorithm continues till convergence.

The BB algorithm must satisfy the following condition to converge to global optimum [49],

Lemma 5 *Any infinite series of successively partitioned regions* $\{T_m\}$ *satisfy,*

$$\lim_{m\to\infty}(\beta(T_m) - \alpha(T_m)) = 0 \tag{5.3}$$

where $\beta(T_m)$ *and* $\alpha(T_m)$ *are the upper and lower bounds of the optimum on* T_m *respectively.*

In a series of successively partitioned regions $\{T_m\}$, each T_{m+1} is a partitioned part of T_m. Figure 5-2 shows a successively partitioned regions.

Given the general frame of the BB algorithm, for an individual optimization problem appropriate algorithms have to be constructed to accomplish each step. The most prominent task is to develop the algorithms for the following three basic operations,

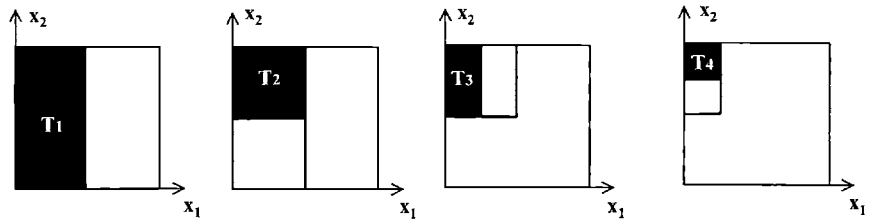

Figure 5-2: Illustration of a Successively Partitioned Series

1. Partition a region into subregions,

2. Calculate the upper bound of the optimum over a subregion,

3. Calculate the lower bound of the optimum over a subregion.

Developing good algorithms to perform these operations are essential for the construction of a decent BB process.

For optimization problems in high dimensional space a BB algorithm might have to search a large number of subregions in each iteration step and result in low efficiency. References [39, 41] reported an algorithm which solves a BMI problem with twelve decision variables in 2422 seconds. Also according to [41], algorithms presented in [47] and [44] have lower performance in the numerical experiments. The BMI associated with the model reduction of a second order system has twelve decision variables. Spending forty minutes on a second order system does not seem to be acceptable. Reference [40] attempted to enhance the efficiency of BB algorithm by reducing the number of subregions. However in this reference an incorrect assumption was made that upper and lower bounds as defined in the reference exist over all subregions[1].

[1]In one of his email communications with the author of this thesis, the author of Reference [40] acknowledges that the algorithm constructed for calculating the upper bound as in the reference may not have solution.

5.3 Branch-and-Bound Procedure for Model Reduction Problem

This section presents a BB algorithm that divides the searched region with respect to μ_i' only. As stated at the end of Chapter 4, the decision variables of a BMI problem associated with the model reduction of an n^{th} order system include n μ_i' and $n(2n+1)$ independent components of $\mathbf{P}$. Therefore for a system whose order is not trivially small, the number of μ_i' is a small fraction of the number of all decision variables. Thus dividing along μ_i' only may result in much less number of subregions in the search.

To facilitate further presentation and the proof, the form of the constraints are adjusted. First, a standard representation of BMI problems [47] is adopted. The constraint (4.23) can be written as,

$$\sum_{j=1}^{n'} p_j \mathbf{G}_j > 0 \tag{5.4}$$

where p_js are the independent components of $\mathbf{P}$, and $\mathbf{G}_j$ are constant matrices with the same dimensions as $\mathbf{P}$. $\mathbf{G}_j(k,l) = 1$ if $P(k,l)$ is p_j and 0 otherwise. Furthermore, for each given problem, without loss of generality p_j can be assumed to be finite. Denote the upper and lower bound of p_j as p_{jsup} and p_{jinf} respectively. The constraint (4.24) can be written as [2][47],

$$\mathbf{M}(\mu_i, p_j, w_{ij}) = \mathbf{F}_{00} + \sum_{i=1}^{n} \mu_i' \mathbf{F}_{i0} + \sum_{j=1}^{n'} p_j \mathbf{F}_{0j} + \sum_{i=1}^{n} \sum_{j=1}^{n'} w_{ij} \mathbf{F}_{ij} < 0 \tag{5.5}$$

where,

$$w_{ij} = \mu_i' p_j \tag{5.6}$$

Matrices $\mathbf{F}_{ij}$ has the same dimension as $\mathbf{M}$. $\mathbf{F}_{00}$ contains terms independent of μ_i, p_j and w_{ij}. $\mathbf{F}_{i0}(k,l)$, $\mathbf{F}_{0j}(k,l)$ and $\mathbf{F}_{ij}(k,l)$, $i,j \neq 0$ are the coefficients of μ_i', p_j and w_{ij}

[2]The purpose of rewriting constraint (4.24) is to separate the linear and nonlinear terms with respect to μ_i' and p_j.

in the (k, l) component of $\mathbf{M}$ respectively. Also denote the matrix whose ij^{th} entry is w_{ij} as $\mathbf{W}$. Second, as shown in Section 5.2, the BB method works on subregions of the overall decision variable space. Therefore instead of using the constraint (4.22), we use,

$$\mu'_{iinf} < \mu'_i < \mu'_{isup},\ i = 1, \ldots, n \tag{5.7}$$

where μ'_{iinf} and μ'_{iisup} delineates the boundary of a specific subregion. Third, the constraint of $\mathbf{P} > 0$ is replaced by the following equivalent constraint,

$$\mu'_{iinf}\left[\sum_{j=1}^{n'} p_j \mathbf{G}_j\right] - \sum_{j=1}^{n'} w_{ij}\mathbf{G}_j < 0 \tag{5.8}$$

$$-\mu'_{isup}\left[\sum_{j=1}^{n'} p_j \mathbf{G}_j\right] + \sum_{j=1}^{n'} w_{ij}\mathbf{G}_j < 0 \quad \forall i \tag{5.9}$$

The equivalence is obvious. In fact, with (5.7) $\mathbf{P} > 0$ is equivalent to,

$$(\mu'_{iinf} - \mu'_i)\left[\sum_{j=1}^{n'} p_j \mathbf{G}_j\right] < 0 \tag{5.10}$$

$$(-\mu'_{isup} + \mu'_i)\left[\sum_{j=1}^{n'} p_j \mathbf{G}_j\right] < 0 \forall i \tag{5.11}$$

Inequalities (5.8) and (5.9) can be obtained by expanding the left hand sides of inequalities (5.10) and (5.11). The significance of inequalities (5.8) and (5.9) will be made clear when proving the convergence of the proposed algorithm. As a summary, after these adjustments the optimization problem on a subregion has the following form,

$$\max L = \sum_{i=1}^{n} \mu'_i \tag{5.12}$$

subject to,

$$\mu'_{iinf} < \mu'_i < \mu'_{isup}, \forall i \tag{5.13}$$

$$\mu'_{iinf}\left[\sum_{j=1}^{n'} p_j \mathbf{G}_j\right] - \sum_{j=1}^{n'} w_{ij}\mathbf{G}_j < 0 \tag{5.14}$$

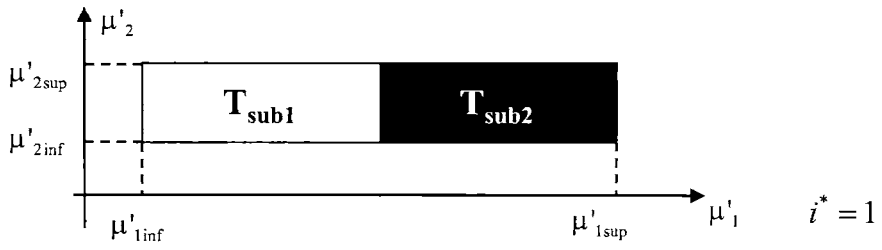

Figure 5-3: Illustration of the $PT(T)$

$$-\mu'_{isup}\left[\sum_{j=1}^{n'} p_j \mathbf{G}_j\right] + \sum_{j=1}^{n'} w_{ij}\mathbf{G}_j < 0 \quad \forall i \tag{5.15}$$

$$\mathbf{M}(\mu_i, p_j, w_{ij}) = \mathbf{F}_{00} + \sum_{i=1}^{n} \mu'_i \mathbf{F}_{i0} + \sum_{j=1}^{n'} p_j \mathbf{F}_{0j} + \sum_{i=1}^{n}\sum_{j=1}^{n'} w_{ij}\mathbf{F}_{ij} < 0 \tag{5.16}$$

$$w_{ij} = \mu'_i p_j \tag{5.17}$$

In this paragraph, the algorithms for the three basic operations are constructed. The algorithm for the partitioning a subregion T is denoted as $PT(T)$. The input to $PT(T)$ is a region T, defined by the inequalities,

$$T = \left[\mu'_{1inf} < \mu'_1 < \mu'_{1sup}, \ldots \mu'_{ninf} < \mu'_n < \mu'_{nsup}\right] \tag{5.18}$$

PT divides T evenly along its longest edge. Mathematically PT generates two subregions T_{sub1} and T_{sub2} that satisfies,

$$T_{sub1} = \left[\mu'_{1inf} < \mu'_1 < \mu'_{1sup}, \ldots, \mu_{i^*inf} < \mu'_i < \frac{\mu_{i^*inf} + \mu_{i^*sup}}{2}, \ldots \mu'_{ninf} < \mu'_n < \mu'_{nsup}\right] \tag{5.19}$$

$$T_{sub2} = \left[\mu'_{1inf} < \mu'_1 < \mu'_{1sup}, \ldots, \frac{\mu_{i^*inf} + \mu_{i^*sup}}{2} < \mu'_i < \mu'_{i^*sup}, \ldots \mu'_{ninf} < \mu'_n < \mu'_{nsup}\right] \tag{5.20}$$

where i^* is the index for $\max_i(\mu'_{isup} - \mu'_{iinf})$. The output of PT is T_{sub1} and T_{sub2}. Figure 5-3 is an illustration of the operation. The algorithm for calculating the upper bound of $\max L$ over T is denoted as $UB(T)$. The input to $UB(T)$ is region T. $UB(T)$ solves the optimization problem consists of (5.12), (5.13), (5.14), (5.15) and

(5.16). The output is the best parameter configuration for $UB(T)$ problem $\{\mu'_{iUB}\}$, the corresponding $\mathbf{P}_{UB}$ and the corresponding maximum $\beta(T) = \sum_{i=1}^{n} \mu'_{iUB}$ if UB is feasible, and an 'infeasible' flag otherwise. UB has one less constraint, namely (5.17), than the original optimization problem. Therefore $\beta(T)$ is greater than or equal to $\max L$ over T, and thus can be used as an upper bound for $\max L$. Furthermore, obviously there is no guarantee for $\max L$ to reach $\beta(T)$, and μ'_{iUB}s do not necessarily satisfy all constraints of the original optimization problem. If $UB(T)$ is infeasible, then the original optimization problem is not feasible on T, since the latter has only more constraints than the former. The algorithm for calculating the lower bound of $\max L$ over T is denoted as $LB(T)$. The inputs to $LB(T)$ are region T and $\mathbf{P}_{UB}$ obtained in $UB(T)$. $LB(T)$ fixes $\mathbf{P}$[3] in (5.14), (5.15) and (5.16) to be $\mathbf{P}_{UB}$ and solves the optimization problem of (5.12), (5.13) and (5.16). The constraints (5.14) and (5.15) is now redundant because $\mathbf{P}_{UB}$ is guaranteed to be positive definite [4]. The outputs are the best parameter configuration for $LB(T)$ problem $\{\mu'_{iLB}\}$ and the corresponding maximum $\alpha(T) = \sum_{i=1}^{n} \mu'_{iLB}$ if LB is feasible, and an 'undetermined' flag otherwise. Since $LB(T)$ has one more constraint than the original optimization problem $\alpha(T)$ is less than or equal to $\max L$. Furthermore, $\{\mu'_{iLB}\}$ is guaranteed to satisfy all constraints of the original problem. Since $LB(T)$ has two more constraints than $UB(T)$, in general the feasibility of $UB(T)$ does not guarantee the feasibility of $LB(T)$.

Since for an arbitrary subregion T, $UB(T)$ and/or $LB(T)$ are not necessarily feasible, new mechanisms be added to the general frame of the BB algorithm to handle

[3]The way $\mathbf{P}$ is calculated and used in the proposed branch-and-bound procedure directly influences the efficiency of the procedure. The efficiency of a branch-and-bound procedure may be higher if, for each subregion, the obtained lower bound is closer to the obtained upper bound, which in turn implies that the search is closer to convergence. The use of the value of $\mathbf{P}$ obtained in the upper bound problem to calculate the lower bound is based on a widely acknowledged speculation in branch-and-bound algorithms[47], that is, the lower bound may have a better chance to be close to the upper bound if the former is generated with the same $\mathbf{P}$ of the latter. If for a specific problem the speculation turns out to be true, the branch-and-bound problem may converge faster. Otherwise, several more partitioning of the involved subregion may be required, which may slow down the convergence procedure.

[4]$\mathbf{P}_{UB}$ is positive definite because it is obtained from problem UB. In problem UB, (5.14) and (5.15) guarantees the positive definiteness of $\mathbf{P}_{UB}$.

such cases. If $UB(T)$ is not feasible, in other words no parameter combination in T satisfies (5.13), (5.14), (5.15) and (5.16) simultaneously, then the original optimization problem, which has one more constraint than $UB(T)$ namely (5.17), is not feasible on T. Consequently T shall be remove from further search. The case for LB is different. Later in the thesis it will be proven that after sufficiently many partitions, feasibility of UB implies feasibility of LB. In other words, for a subregion T not removed by the algorithm, when the volume of T is sufficiently small LB is always feasible. This means when $LB(T)$ is infeasible T shall be kept in the partitioning and search process. Example 1 illustrates the issue of the feasibility of UB and LB.

With the above algorithms the overall BB process can be constructed. The meanings of some new symbols are listed below. T_{kl} is a subregion indexed l at the k^{th} iteration of the BB process. $\Phi_k = \{T_{kl}\}$ is the set of subregions at Step k. $\lambda_k = \max_{argl}(\alpha(T_{kl}))$ is the largest value of L achieved in Step k, since as pointed out in the last paragraph, α is the sum of a set of parameters that satisfy all constraints of the original optimization problem. Now the steps of the BB process can be listed as following,

Step 0 Set $T_{11} = [0 < \mu'_1 < H, \ldots, 0 < \mu'_n < H]$, $\lambda_0 = 0$, $\Phi_1 = T_{11}$ and $k = 0$. Set the tolerance of the algorithm $\epsilon_a > 0$.

Step 1 Set $k = k + 1$. For each $T_{kl} \in \Phi_k$, solve $UB(T_{kl})$. If $UB(T_{kl})$ is infeasible, remove T_{kl}. Otherwise obtain $\beta(T_{kl})$ and the corresponding $\mathbf{P}_{UB}$. Then solve $LB(T_{kl})$. If $LB(T_{kl})$ is infeasible, mark T_{kl} as 'undetermined'. Otherwise obtain $\alpha(T_{kl})$. Set $\lambda_k = \max_{l}\{\alpha(T_{kl})\}$, and the corresponding $\{\mu'_1, \ldots \mu'_n\}$ are labeled $\{\mu'_{1k}, \ldots, \mu'_{nk}\}$.

Step 2 In Φ_k, delete all T_{kl}'s such that $\beta(T_{kl}) \leq \lambda_k + \epsilon_a$. Denote the set of the remaining regions R_k. If $R_k = \phi$, the algorithm terminates. λ_k is the ϵ-suboptimal value with corresponding $\{\mu'_{1k}, \ldots, \mu'_{nk}\}$. Otherwise, continue to Step 3.

Step 3 In R_k choose T^* that corresponds to $\max_{argl}(\beta(T_{kl}) - \alpha(T_{kl}))$. Also, choose all 'undetermined' T_{kl}s. Denote the set of all the chosen regions $\{T_h\}$ where h is

the index. Set $\Phi_{k+1} = \{R_k \setminus \{T_h\}\} \cup \{\bigcup_h (PT(T_h))\}$. Go to Step 1.

The proposed BB method automatically seeks the combination of the system parameters that contains as many μ_i' close to H as possible. This is different from most existing model reduction procedures in physical domain, which tries to remove physical components one by one. As shown by an example in the previous chapter, the former approach may lead to simpler reduced models.

5.4 Proof of Convergence

This section proves with Lemma 5 that the algorithm converges to global ϵ-suboptimum . The very first step shall be the proof of the existence of $\beta(T_m)$ and $\alpha(T_m)$, i.e. the feasibility of $UB(T_m)$ and $LB(T_m)$, when m is sufficiently large. The proof is necessary because, as pointed out in Section 5.3, in general the feasibility of UB and LB are not guaranteed over a given region.

The following lemma is useful.

Lemma 6 *Given the partitioning rule PT, any infinite successively partitioned series $\{T_m\}$ satisfies,*

$$\forall \epsilon > 0, \exists \xi(\epsilon) \ s.t. \ \forall m > \xi(\epsilon) \ \mu'_{isup} - \mu'_{iinf} < \epsilon \ \forall i \tag{5.21}$$

Physically, Lemma 6 says that after sufficiently many partitions, the edge length of the region being cut becomes arbitrarily small. This lemma is obviously true.

Now the proof of the feasibility of UB and LB for sufficiently large m is presented. The feasibility of $UB(T_m)$ is trivially true because the algorithm removes any subregion with infeasible UB. So for a *infinite* successively partitioned series $UB(T_m)$ is feasible $\forall m$. Given the feasibility of $UB(T_m)$, the feasibility of LB can be proved by showing,

Theorem 3 *With the partitioning rule PT, when m is sufficiently large if $UB(T_m)$ is feasible then $LB(T_m)$ is feasible.*

Proof

The proof is constructed in two stages. In the first stage, it is shown that when m is sufficiently large, w_{ijUB} is arbitrarily close to $\mu'_{iUB}p_{jUB}$. In the second stage, it is shown that when w_{ijUB} is sufficiently close to $\mu'_{iUB}p_{jUB}$, if UB is feasible LB is feasible.

Now let us begin with the first stage. According to Lemma 6 when m is sufficiently large the following equations hold for arbitrarily small $\epsilon_i > 0$,

$$\mu'_{iUB} = \mu'_{iinf} + \epsilon_i \tag{5.22}$$

On the other hand, the solution of UB must satisfy the constraint (5.14). According to [40], (5.14) leads to,

$$\mu'_{iinf}p_{jUB} - w_{ijUB} - \mu'_{iinf}p_{jinf} + p_{jinf}\mu'_{iUB} < 0 \tag{5.23}$$

$$\mu'_{iinf}p_{jsup} - \mu'_{iUB}p_{jsup} - \mu'_{iinf}p_{jUB} + w_{ijUB} < 0 \tag{5.24}$$

Substitute (5.22) into (5.23) and (5.24) one gets,

$$\mu'_{iUB}p_{jUB} + \epsilon_i(p_{jinf} - p_{jUB}) < w_{ijUB} < \mu'_{iUB}p_{jUB} + \epsilon_i(p_{jsup} - p_{jUB}) \tag{5.25}$$

which leads to,

$$w_{ijUB} = \mu'_{iUB}p_{jUB} + \epsilon'_i \tag{5.26}$$

where $|\epsilon'_i|$ is arbitrarily small.

Equation (5.26) indicates that w_{ijUB} and $\mu'_{iUB}p_{jUB}$ are arbitrarily close. Based on this one can prove if UB is feasible then LB is feasible. In fact, assume UB is

feasible and LB is not feasible, i.e. $\forall \mu'_i \in (\mu'_{iinf}, \mu'_{isup})$, one gets[5]

$$\mathbf{F}_{00} + \sum_{i=1}^{n} \mu'_i \mathbf{F}_{i0} + \sum_{j=1}^{n'} p_{jUB} \mathbf{F}_{0j} + \sum_{i=1}^{n} \sum_{j=1}^{n'} (\mu'_i p_{jUB}) \mathbf{F}_{ij} > 0 \tag{5.27}$$

which leads to (due to $\mu'_{iUB} \in (\mu'_{iinf}, \mu'_{isup})$),

$$\mathbf{F}_{00} + \sum_{i=1}^{n} \mu'_{iUB} \mathbf{F}_{i0} + \sum_{j=1}^{n'} p_{jUB} \mathbf{F}_{0j} + \sum_{i=1}^{n} \sum_{j=1}^{n'} (\mu'_{iUB} p_{jUB}) \mathbf{F}_{ij} > 0 \tag{5.28}$$

Then due to continuity for sufficiently small ϵ',

$$\mathbf{F}_{00} + \sum_{i=1}^{n} \mu'_{iUB} \mathbf{F}_{i0} + \sum_{j=1}^{n'} p_{jUB} \mathbf{F}_{0j} + \sum_{i=1}^{n} \sum_{j=1}^{n'} (\mu'_{iUB} p_{jUB} + \epsilon') \mathbf{F}_{ij} > 0 \tag{5.29}$$

Inequality (5.29) indicates that UB is infeasible. This leads to a contradiction to our assumption that UB is feasible. As a conclusion, if UB is feasible then LB is feasible.

End of Proof

Given the result of Theorem 3 it is straight forward to prove $\lim_{m \to \infty} (\beta(T_m) - \alpha(T_m)) = 0$, i.e.

Theorem 4 *In an infinite successively partitioned series of* $\{T_m\}$, $\forall \epsilon > 0, \exists \xi(\epsilon)$ *such that* $\forall m > \xi(\epsilon), \beta(T_m) - \alpha(T_m) < \epsilon$.

Proof

According to Lemma 6, $\forall \epsilon_0 > 0, \exists \xi'(\epsilon_0)$, such that $\forall m > \xi'(\epsilon_0)$, $\mu'_{isup} - \mu'_{iinf} < \epsilon_0 \ \forall i$. Since $J = \sum_{i=1}^{n} \mu'_i$, one gets $\beta(T_m) - \alpha(T_m) < n\epsilon_0 \equiv \epsilon$. One can further set $\xi'(\epsilon_0) = \xi'(\frac{\epsilon}{n}) \equiv \xi(\epsilon)$. Then $\forall \epsilon > 0, \exists \xi(\epsilon)$, such that $\forall m > \xi(\epsilon)$, $\beta(T_m) - \alpha(T_m) < \epsilon$.

End of Proof

Theorem 4 shows the proposed algorithm satisfies the requirement of Lemma 5. Therefore the algorithm converges to global ϵ-optimum [6].

[5] As stated in Section 4.3.2, equality sign is not relevant in this optimization problem.

[6] The efficiency of the calculation highly depends on the specific problem. One thing worthy of pointing out is, it has been proven in the literature that *in the worst case*, the complexity of a BMI problem is proportional to the exponential of its size[46].

5.5 Summary

This chapter proposes a BB based algorithm for solving the BMI optimization problem associated with model reduction. The contribution of this section can be summarized as,

- Constructed a BB algorithm for model reduction in physical domain. The algorithm partitions along system parameters only.
  - Added to the general frame of the BB algorithm the processes for handling subregions with infeasible UB and LB problems.
  - Constructed a BB algorithm for model order reduction in physical domain.
- Proved that the proposed algorithm converges to global ϵ-suboptimum.
  - Proved that after sufficiently many partitions, the feasibility of UB leads to the feasibility of LB.
  - Proved with Lemma 5 that the proposed algorithm converges to global ϵ-optimum.

Chapter 6

Examples

6.1 Example 1: A Generator

The purpose of this example is to use graphs to show the convergence procedure of the proposed BB algorithm.

The system under consideration is shown in Figure 6-1 and its bond graph model is shown in Figure 6-2. The accuracy requirement is $\gamma_p < 0.1$. The range of search is $\frac{1}{I_{1g}} = \mu_1' \in (0, 500)$ and $\frac{1}{I_{2g}} = \mu_2' \in (0, 500)$. The corresponding BMI problem has twelve decision variables, which include μ_1', μ_2' and ten independent elements of $\mathbf{P}$.

Since only two independent system parameters are involved in this example, graphs can be used to show the converge process. The specific process recorded

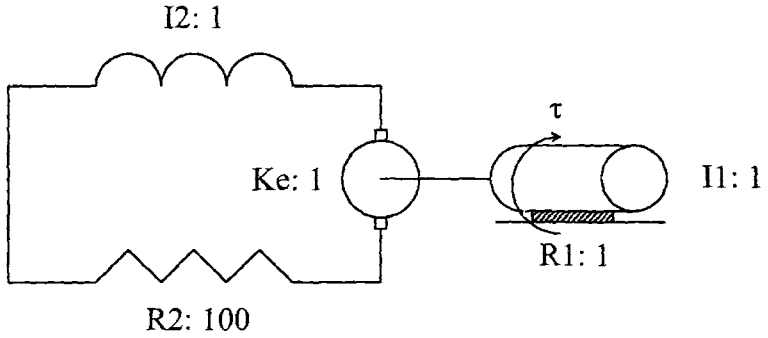

Figure 6-1: A Generator System

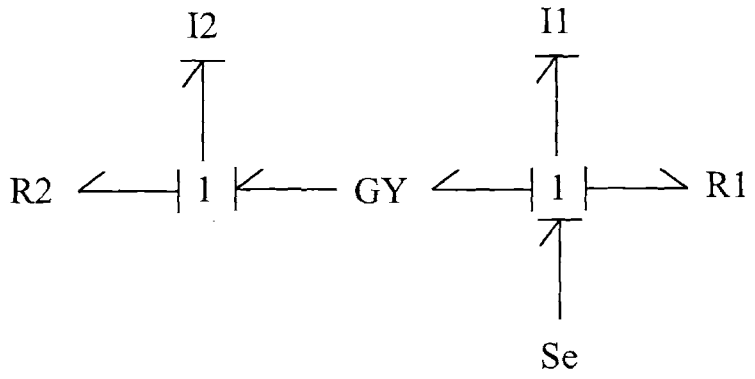

Figure 6-2: Bond Graph Model of a Generator System

in Figure 6-6 through Figure 6-9 includes ten iterations. Each figure shows the state of the subregions at the beginning of an iteration, along with a short explanation of the contents of the figure. White blocks are the subregions that have been removed, grey blocks are the remaining 'undetermined' subregions and the black blocks are the regions whose associated LB problem was found feasible during the previous iteration. In these figures, the horizontal axis is for μ_1' the vertical axis is for μ_2'. The search range of μ_1' and μ_2' are set to be $[0, 500]$.

On the performance aspect, the algorithm converges in 41.9225 seconds and 10 iterations.

The result is $\mu_1' = 0.9634$ and $\mu_2' = 491.0155$. This result shows that I_2 can be removed and I_1 shall be set to $\frac{1}{0.9634} = 1.0380$. The reduced model and the corresponding bond graph are shown in Figure 6-3 and 6-4 respectively. The frequency responses of the original system and the reduced system are plotted in Figure 6-5. The two responses are almost identical.

This example also demonstrates that, as pointed out in Section 5.3, for a given subregion UB and/or LB is not necessarily feasible. In fact, as shown in Figure 6-7, UB is infeasible over the region of $\{0 < \mu_1' < 500, 0 < \mu_2' < 500$. Denote this subregion as $\mathcal{T}$. Since the constraints of UB is a subset of the constraints of LB, LB is also infeasible on $\mathcal{T}$.

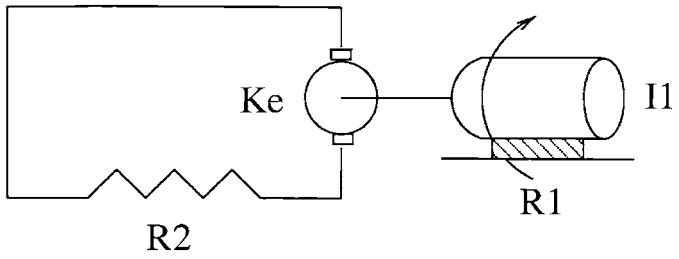

Figure 6-3: Simplified Generator System

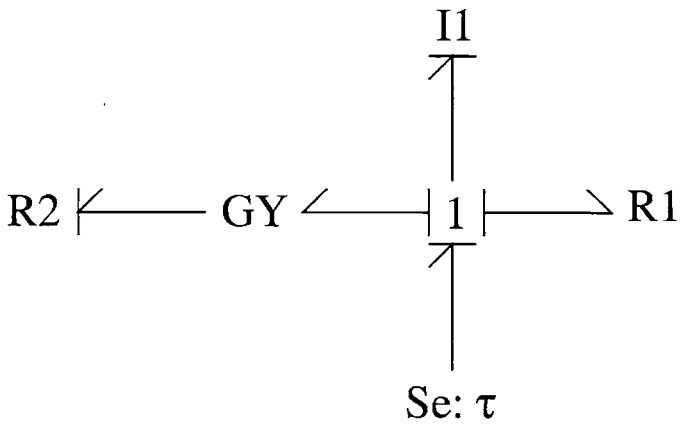

Figure 6-4: Simplified Bond Graph Model of a Generator System

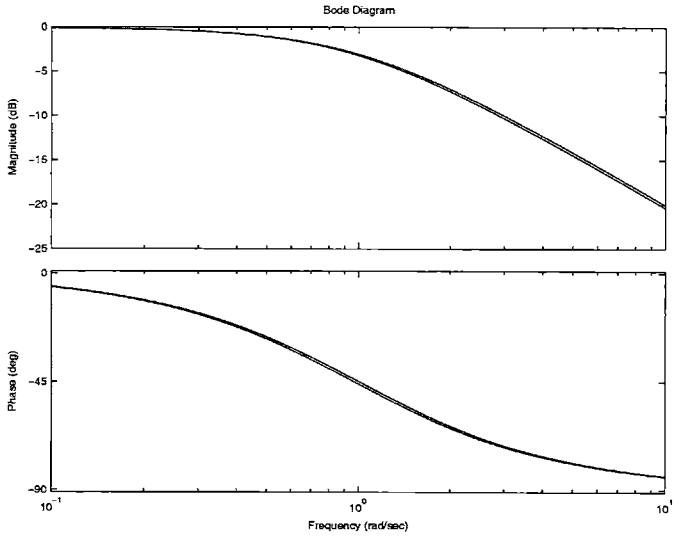

Figure 6-5: Frequency Responses of the Original and the Reduce Model

1st Iteration

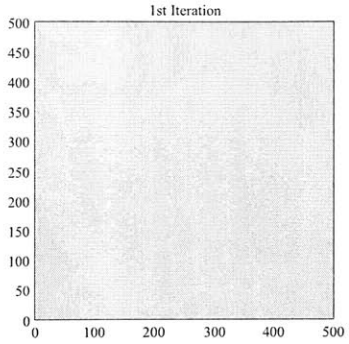

Starting Point: Area of T_0

2nd Iteration

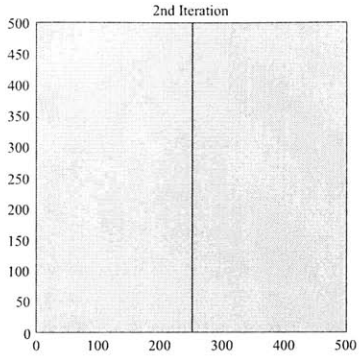

2nd Iteration: T_0 split.

Figure 6-6: Iteration of BB Procedure

3rd Iteration

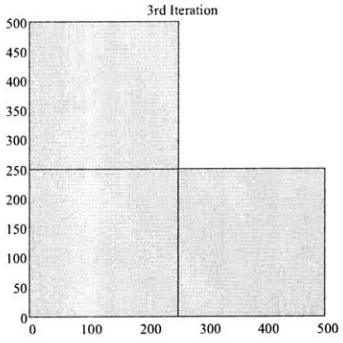

3rd Iteration: One quarter of total area removed for infeasibility of UB

4th Iteration

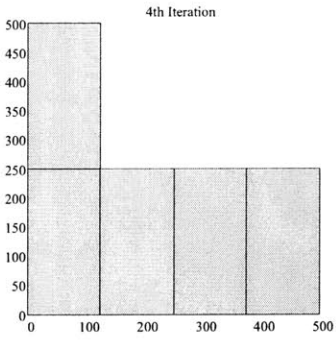

4th Iteration: more areas removed for infeasibility of UB.

Figure 6-7: Iteration of BB Procedure

7th Iteration

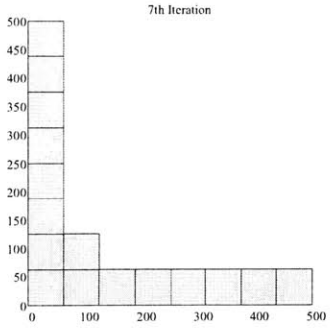

7th Iteration: Three quarters of total area removed for infeasibility of UB.

8th Iteration

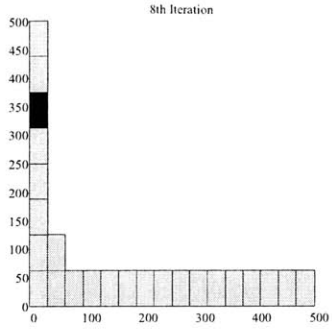

8th Iteration: An area feasible to LB found. Many areas will be removed because upper bound of L over them is now less than λ.

Figure 6-8: Iteration of BB Procedure

9th Iteration

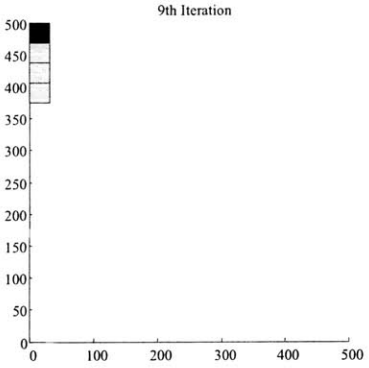

9th Iteration: Many areas removed. A new area feasible to LB found.

10th Iteration

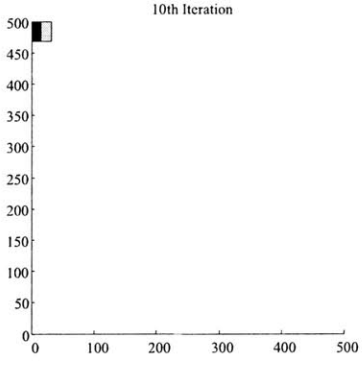

10th Iteration: More areas removed. A area feasible to LB found. Algorithm terminates after this iteration.

Figure 6-9: Iteration of BB Procedure

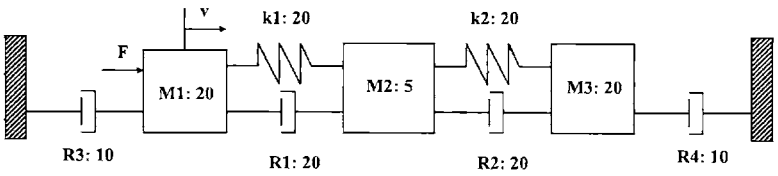

Figure 6-10: Bond Graph Model of a Fifth-Order System

6.2 Example 2: A Fifth-Order System

This example illustrates the use of the proposed model reduction procedure for a more complex system. The system under consideration is shown in Figure 6-10. The accuracy requirement is $\gamma_p < 0.01$. The $\mathbf{J}_A$, $\mathbf{B}$, $\mathbf{J}_C$ and $\mathbf{D}$ matrices are,

$$
\begin{aligned}
\mathbf{J}_A &= \begin{bmatrix} -(R_1+R_3) & R_1 & 0 & -1 & 0 \\ R_1 & -(R_1+R_2) & R_2 & 1 & -1 \\ 0 & R2 & -(R_2+R_4) & 0 & 1 \\ 1 & -1 & 0 & 0 & 0 \\ 0 & 1 & -1 & 0 & 0 \end{bmatrix} \\
\mathbf{B} &= \begin{bmatrix} 1 & 0 & 0 & 0 & 0 \end{bmatrix}^T \\
\mathbf{J}_C &= \begin{bmatrix} 1 & 0 & 0 & 0 & 0 \end{bmatrix} \\
\mathbf{D} &= 0
\end{aligned} \tag{6.1}
$$

Let us first try to approach the problem by inspection. The parameters of the system components are in the same order of magnitude, so no component is obviously redundant. Furthermore, the poles and zeros of the system are $[-7.9929, -1.1305, -0.7500+0.6614i, -0.7500-0.6614i, -1.1305, -0.4466]$ and $[-7.4161, -1.1462, -0.4688+0.5007i, -0.4688-0.5007i]$ respectively. There is one very close pole/zero pair, which is -1.1305/-1.1462. So one may suspect mathematically the model can be reduced to a fourth-order one. At the same time, since all the system parameters are of the same order of magnitude, it is difficult to identify which components or combination of components make major

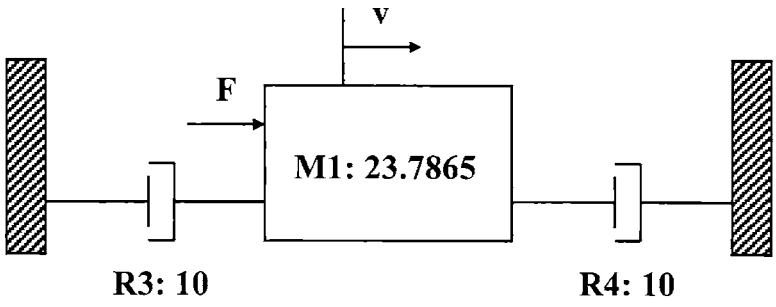

Figure 6-11: Reduced System

contribution to this pole/zero pair.

Now let us apply the procedure presented in this thesis. Define the μ_i' as follows, $\mu_1' = \frac{1}{I_{1g}}$, $\mu_2' = \frac{1}{I_{2g}}$, $mu_3' = \frac{1}{I_{3g}}$, $\mu_4' = \frac{1}{C_{1g}}$, $\mu_5' = \frac{1}{C_{2g}}$. The range of search is $\mu_i' \in (0, 1000)$.

The proposed procedure provides a reduced system of first order! The procedure gets the following result, $\mu_1' = 0.0420$, $\mu_2' = 999.8186$, $\mu_3' = 999.8325$, $\mu_4' = 991.1318$ and $\mu_5' = 954.6731$. These results indicate I_2, I_3, C_1 as well as C_2 can be removed, and the resultant model is shown in Figure 6-11.

The H_∞ norm of the error model is 0.009. The frequency response of the original model and the reduced model are shown in Figure 6-12.

Some may wonder why the reduced model has a mass of 23.8, instead of the summation of the masses of the original system, which is 45. One explanation comes from the bode plot of the original system shown with dashed lines in figure 6-12. From the structure of the original system, one can see that the response at the extremely low frequency is solely determined by R_3 and R_4, which totals forty. The parameters of these resistances are not being changed, since the proposed procedure works on the parameters of the energy storage elements only. At the same time, despite of the fact that the frequency response of the original system has some ripples, its overall shape is quite close to the frequency response of a first order system, with break-off frequency at about 1rad/sec. Thus it makes sense for the reduced model to have an overall mass of about forty.

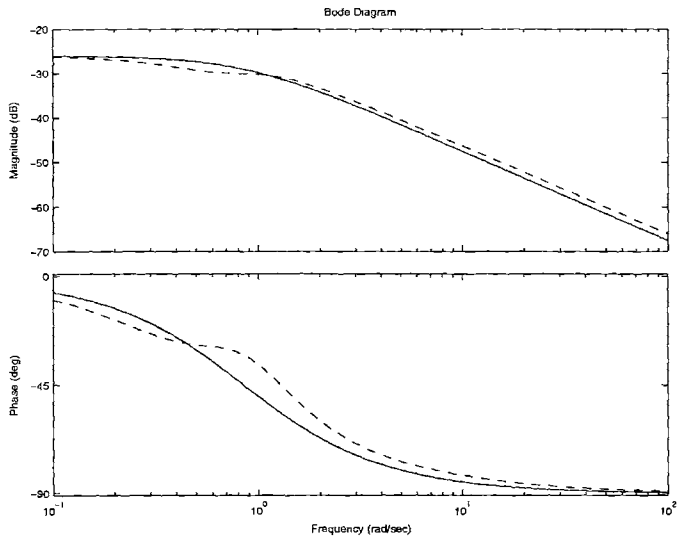

Figure 6-12: Frequency Response of the Original (Dashed Line) and the Reduced (Solid Line) Systems

This example also shows that the proposed model reduction procedure identifies the contribution of the combination of energy storage elements to the system dynamic behavior, rather than tries to remove the components one by one. In fact, it is difficult to point out, in this example, which component makes major contribution to which eigenvalue. The model reduction procedure 'summarizes' the contribution of all components and use the minimum number of energy storage elements to realize the transfer matrix (in this case a transfer function) of the original system.

6.3 Example 3: Error Model with an Output Filter

This example illustrate the use of input/output filters. Consider the system in Figure 6-13. Suppose the frequency range of interest is $\omega < 1 rad/sec$. The magnitude of the frequency response within this range is greater or equal to 0.05. Let us chose γ_p be 30solid lines.

A sixth-order Butterworth filter with cut-off frequency of $1 rad/sec$ is used as the

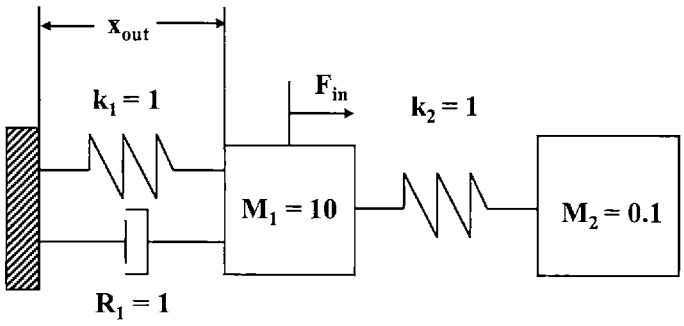

Figure 6-13: A Fourth-Order System

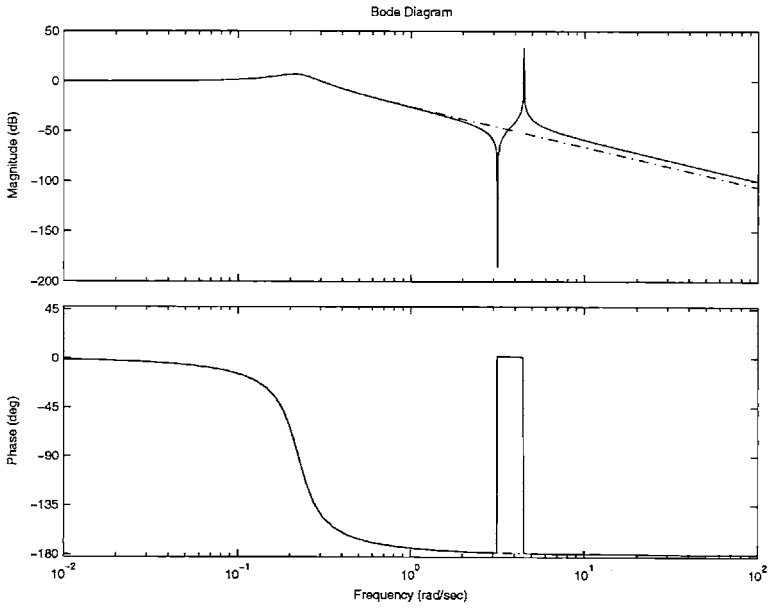

Figure 6-14: Frequency Response of the Fourth-Order System: Solid: Original, Dashed: Reduced

output filter. With the notations in (4.25), its state space realization can be written as,

$$
\begin{aligned}
\mathbf{A}_{out} &= \begin{bmatrix} -3.8637 & -1.8660 & -1.1427 & -0.9330 & -0.4830 & -0.1250 \\ 4.0000 & 0 & 0 & 0 & 0 & 0 \\ 0 & 2.0000 & 0 & 0 & 0 & 0 \\ 0 & 0 & 1.0000 & 0 & 0 & 0 \\ 0 & 0 & 0 & 1.0000 & 0 & 0 \\ 0 & 0 & 0 & 0 & 1.0000 & 0 \end{bmatrix} \\
\mathbf{B}_{out} &= \begin{bmatrix} 0.2500 & 0 & 0 & 0 & 0 & 0 \end{bmatrix}^T \\
\mathbf{C}_o ut &= \begin{bmatrix} 0 & 0 & 0 & 0 & 0 & 0.5000 \end{bmatrix} \\
\mathbf{D}_o ut &= 0
\end{aligned} \tag{6.2}
$$

The proposed algorithm gives the reduced model shown in Figure 6-15. The corresponding frequency response is shown in Figure 6-14 in dashed lines. The response matches that of the original model up to about $1.5 rad/sec$ as required.

The H_∞ norm of the error model is 0.014, which is less than the required error margin of 0.015.

6.4 Example 4: Model Assembly

In contemporary engineering practice, system assembly is an important part of system design. Many complex systems are assembled with the subsystems which are off-the-shelf products. How to build simplest model for such systems is an interesting problem.

One may have less freedom in the modeling of such assembled systems. Often off-the-shelf products come with models, developed by the suppliers, whose parameters are not subject to change or omission. In such cases, the best one can do is to decide which self-designed components and/or the related physical phenomenon shall be included in the model. Such kind of problems are sometimes referred to as model

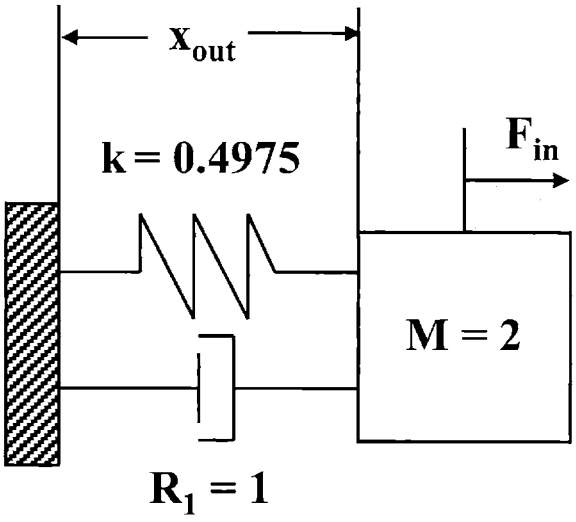

Figure 6-15: Reduced System

assembly problems.

Model assembly problem is in fact a variation of model reduction problem. The only difference is that now only part of the parameter space, i.e. the parameter space corresponding to the self-designed energy storage elements, needs to be searched. The optimization procedure developed in the previous chapters for model reduction can be directly applied to model assembly problems.

Consider the system in Figure 6-16 with all the component parameters. This system is composed of a motor and a mechanical system. The shaft of the motor pulls a mass horizontally via a cable with compliance and resistance. Assume the friction between the mass and the ground is negligible. Suppose the parameters of the motor are given and are not subject to change. Let the input be the voltage of the electric source, and the output is the current[1] in the circuit. The problem is to identify the relevance of the mechanical components, namely the inertia of the shaft, spring and the mass.

Choose as the state variables the generalized momenta associated with inductance I, inertia J, mass M as well as the generalized displacement associated with the

[1]The current is useful when, for example, choosing an appropriate power amplifier.

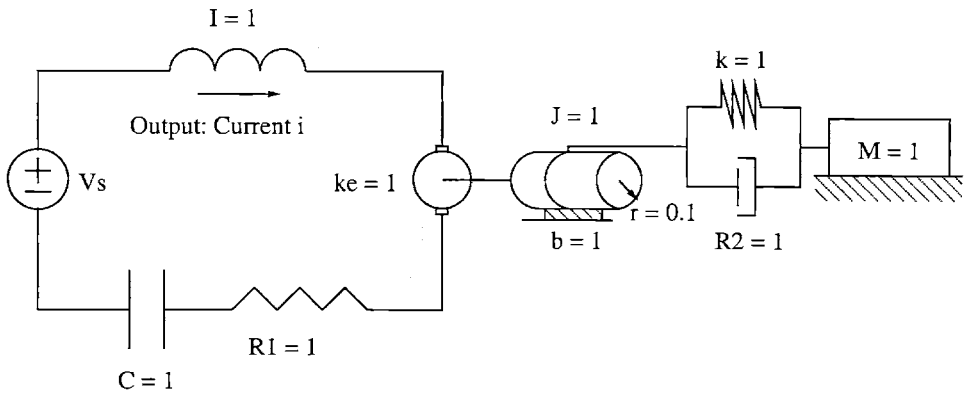

Figure 6-16: A Motor-Load System

capacitance C and spring K. Denote the state variables as p_1, p_2, p_3, q_1 and q_2. Denote the inverse of mechanical side system parameters $\frac{1}{J}$, $\frac{1}{M}$ and k as μ_1', μ_2' and μ_3' respectively. With the following state vector $\mathbf{x} = [p_1, p_2, p_3, q_1, q_2]^T$, the system parameterization can be found as,

$$\mathbf{A}_g = \begin{bmatrix} -1 & -1 & 0 & -1 & 0 \\ 1 & \frac{-1}{100} - \frac{1}{10} & 0 & \frac{1}{10} & \\ 0 & \frac{1}{10} & -1 & 0 & 1 \\ 1 & 0 & 0 & 0 & 0 \\ 0 & \frac{1}{10} & -1 & 0 & 0 \end{bmatrix} \begin{bmatrix} 1 & 0 & 0 & 0 & 0 \\ 0 & \mu_1' & 0 & 0 & 0 \\ 0 & 0 & \mu_2' & 0 & 0 \\ 0 & 0 & 0 & 1 & 0 \\ 0 & 0 & 0 & 0 & \mu_3' \end{bmatrix} \tag{6.3}$$

$$\mathbf{B}_g = \begin{bmatrix} 1 & 0 & 0 & 0 & 0 \end{bmatrix}^T \tag{6.4}$$

$$\mathbf{C}_g = \begin{bmatrix} 1 & 0 & 0 & 0 & 0 \end{bmatrix} \tag{6.5}$$

$$\mathbf{D}_g = 0 \tag{6.6}$$

For this example, the error margin is chosen to be a value much smaller than the peak value of the frequency response. Specifically, γ_p is chosen to be 0.003, which is less than 1search be $0 < \mu_i' < 1000$. The optimization procedure finds the mass M and the spring k can be removed while the inertia of the shaft changes very little. The resultant H_∞ norm is 0.0021.

This result makes physical sense. The shaft of the motor has a quite small radius,

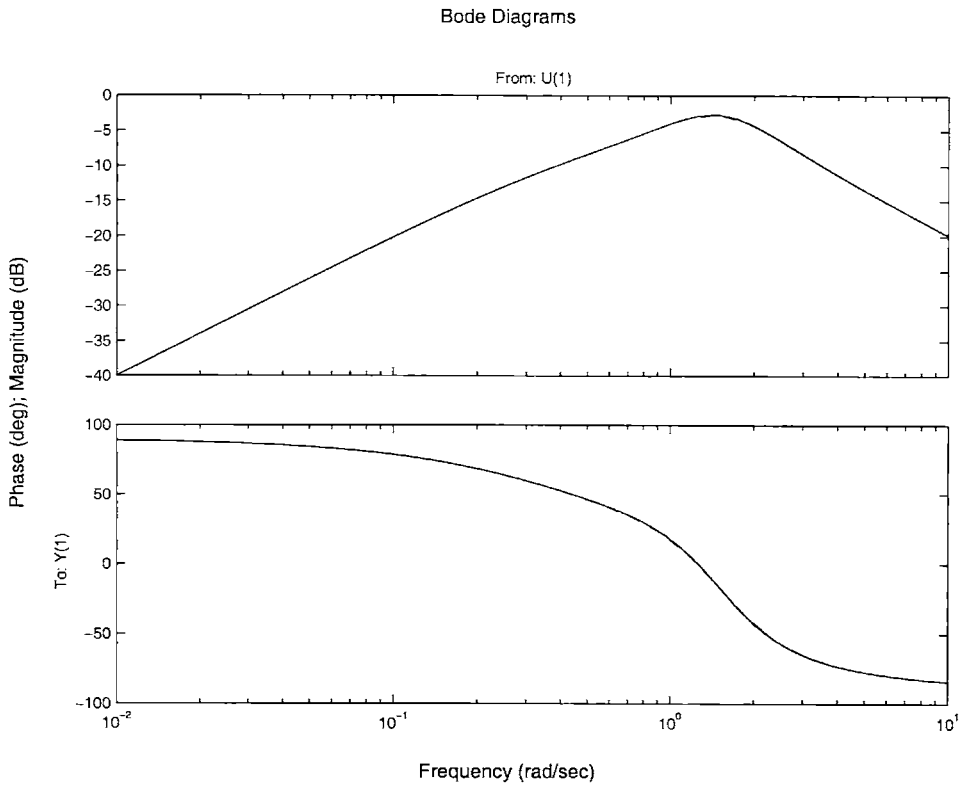

Figure 6-17: Bode Plot of the Original (Solid Lines) and the Reduced (Dashed Lines) System

therefore the numerical value of the output torque of the motor is very small compare to that of the force on the cable. Consequently the influence of the dynamics of the mechanical side on the electric side is quite small.

The bode plots of the original and the reduced system are shown in Figure 6-17. The two responses are almost identical.

Chapter 7

Conclusion and Recommendations for Further Research

The major work of this thesis can be summarized in one sentence: based on the intuition obtained from the recalibration of the fundamentals, and utilizing results of contemporary research, a rigorous framework and an algorithm with satisfactory efficiency are developed for model reduction problem.

The most important step in the research is perhaps expanding the scope of model reduction to include the adjustment of all system parameters. Physically, this expansion is reasonable because many components may make contribution to the dynamics of the overall system as a whole, due to the coupling among them. Consequently, much simpler model may be obtained when the parameters of all components are subject to change. Furthermore, the idea of searching the whole parameter space for the best model leads to the understanding that model reduction in the physical domain is essentially an optimization problem.

Formulating the model reduction in the physical domain as an optimization problem is another significant step. One major achievement in this step is the mathematical abstraction of the goal of model reduction, i.e. the construction of a index function that reaches its optimum when as many energy storage elements as possible are set to be arbitrarily small. Also, it is proven that an element is removable if its parameter can be set to be a sufficiently small positive value. Consequently, no

causality change happens during the search process and therefore one does not have to rederive system equations for different candidate reduced models. The formulation of model reduction as an optimization problem opens up the gate for applying competent mathematical tools for model reduction. In fact, this formulation relates the model reduction problem with one of the most attractive frontiers of in control and dynamics area, which is the solving of BMI problem. Future progresses in BMI research can be directly exploited for model reduction purpose.

The discussion on the power-based methods is another interesting part of the thesis work. The author has not seen any continuation of the effort for developing variations of such methods, which started in 1988 and produced several publications, since 1999, the year when the three counter examples were published in [1] and [5].

In this thesis, a BB procedure is proposed for solving the BMI problem associated with model reduction. The proof of its convergence to global maximum assures the simplest model, for the model reduction problem discussed in this thesis, can be achieved.

The thesis work also brings up some interesting topics for future research. One is to include the dissipation elements in the model reduction procedure. At this time, the simplest parameterization with both dissipation and energy storage elements gives a 'trilinear' matrix inequality constraint(See B). Although in principle BB algorithm can be used to solve such kind of problems, the efficiency could be low due to the mathematical complicity. A better form of parameterization may be the key. Another possible research topic is to develop solutions for the associated BMI problem with better efficiency. The BMI problem involved in model reduction is quite structured, which provides the possibility of developing specialized high efficiency algorithms. Also, model reduction criteria other than H_∞ norm shall be investigated for various applications.

As a summary, the contributions of this paper include,

- Constructed three counter examples for power-based model reduction procedure.

- Expanded the scope of model reduction in physical domain to include the adjustment of all system parameters.
- Developed a fully automated model reduction procedure that guarantees the error of the reduced model in H_∞ norm.
  - Formulated model reduction problem as an optimization problem with BMI constraints.
  - Developed a BB algorithm for the optimization problem associated with model reduction. Proved the convergence of the algorithm to the global optimum.

And the recommendations for future work include,

- Include dissipation elements in future model reduction procedure.
- Enhance the efficiency for solving BMI problems.
- Investigate error norms other than H_∞.

Appendix A

List of Symbols

[1]

n: Order of the original system,

$P_i(t)$: Power flow associated with the bond labeled i

$\mathcal{P}_i(t)$: RMS of $P_i(t)$, $\mathcal{P}_i = \sqrt{\frac{1}{T}\int_0^T P_i^2(t)dt}$

AI_i: Activity index of bond i, defined as $AI_i = \frac{\int_0^T |P_i(t)|dt}{\Sigma_{j=1}^n \int_0^T |P_i(t)|dt}$,

$\mathbf{G}$: Transfer matrix of the original model,

$\mathbf{G}_r$: Transfer matrix of the reduced model,

$\mathbf{G}_{error}$: Transfer matrix of the error model as in Figure 3-9,

$e_o(t)$: Output of the error model as a function of time,

γ_p: Prescribed error margin. The transfer matrix of the reduced model shall satisfy $\|G - G_r\|_\infty < \gamma_p$,

SYS_o: Original system,

SYS_g: Generalized system. A system with the same structure of the original system while the parameters of the energy storage elements can be chosen aribitrarily,

μ_i: The parameter of the i^{th} energy storage element in the original system,

μ_{gi}: The parameter of the i^{th} energy storage element in the generalized system,

$\mathbf{A}_p, \mathbf{B}_p, \mathbf{C}_p, \mathbf{D}_p$: State space representation of the generalized system with the flow associated with the inertances and the efforts associated with the capacitances as the

[1] Standard symbols, such as ω for angular frequency, is not listed.

state variables,

μ_i': Inverse of μ_{gi},

L: Index function for the optimization problem associated with model reduction,

H: The artificial upper bound for μ_i'. Chosen to be a sufficiently large number,

η: Scaling factor used for the search of H,

$\mathbf{A}, \mathbf{B}, \mathbf{C}, \mathbf{D}$: State space representation of the original model, with the generalized momenta associated with the inertances and the generalized displacements associated with the capacitances as state variables,

$\mathbf{A}_g, \mathbf{B}_g, \mathbf{C}_g, \mathbf{D}_g$: State space representation of the generalized model, with the generalized momenta associated with the inertances and the generalized displacements associated with the capacitances as state variables. Since $\mathbf{B}_g$ and $\mathbf{D}_g$ are independent of system parameters one has $\mathbf{B}_g = \mathbf{B}$ and $\mathbf{D}_g = \mathbf{D}$,

$\mathbf{E}_g$: Parameter matrix for the generalized model, $\mathbf{E}_g = \begin{bmatrix} \mu_1' & & \\ & \ddots & \\ & & \mu_n' \end{bmatrix}$,

$\mathbf{J}_A$: Matrix that relates $\mathbf{A}_g$ and $\mathbf{E}_g$, $\mathbf{A}_g = \mathbf{J}_A \mathbf{E}_g$,

$\mathbf{J}_C$: Matrix that relates $\mathbf{C}_g$ and $\mathbf{E}_g$, $\mathbf{C}_g = \mathbf{J}_C \mathbf{E}_g$,

$\mathbf{P}$: A positive definite matrix,

$\mathbf{M}$: A matrix that contains the BMI constraints of the optimization problem associated with model reduction,

$\mathbf{A}_{in}, \mathbf{B}_{in}, \mathbf{C}_{in}, \mathbf{D}_{in}$: A state space realization of the input filter of the error model as in Figure 3-10,

$\mathbf{A}_{out}, \mathbf{B}_{out}, \mathbf{C}_{out}, \mathbf{D}_{out}$: A state space realization of the output filter of the error model as in Figure 3-10,

$\mathbf{A}_{error}, \mathbf{B}_{error}, \mathbf{C}_{error}, \mathbf{D}_{error}$: A state space realization of the error model as in Figure 3-10, $\mathbf{A}_{error0}, \mathbf{B}_{error0}, \mathbf{C}_{error0}, \mathbf{D}_{error0}$: A state space realization of the error model as in Figure 3-9,

$\{T_m\}$: A series of successively partitioned region in a BB process,

$\beta(T)$: Upper bound of the optimum over region T,

$\alpha(T)$: Lower bound of the optimum over region T,

p_j: Independent components of $\mathbf{P}$. $\mathbf{G}_j$: Constant matrix, $\mathbf{G}_j(k,l) = 1$ if $P(k,l) = p_j$ and 0 otherwise,

w_{ij}: $w_{ij} = \mu_i' p_j$,

$\mathbf{F}_{ij}$: Constant matrices, $\mathbf{F}_{00}$ contains terms independent of μ_i, p_j and w_{ij}. $\mathbf{F}_{i0}(k,l)$, $\mathbf{F}_{0j}(k,l)$ and $\mathbf{F}_{ij}(k,l)$, $i,j \neq 0$ are the coefficients of μ_i', p_j and w_{ij} in the (k,l) component of $\mathbf{M}$ respectively,

$\mathbf{W}$: A matrix whose (i,j) component is w_{ij},

μ_{iinf}', μ_{isup}': Upper and Lower bound of μ_i' over a subregion,

T: A subregion in BB algorithm,

$UB(T), LB(T)$: The algorithm for calculating the upper/lower bound of the optimization problem associated with model reduction over region T,

$PT(T)$: The algorithm for partitioning region T,

T_{kl}: A subregion indexed l at the k^{th} iteration of the BB algorithm,

Φ_k: The set of all T_{kl} at the k^{th} iteration,

λ_k: $\lambda_k = \max_{arg\ l}(\alpha(T_{kl}))$,

ϵ_a: Tolerance of the BB algorithm,

$\mu_{iUB}', p_{jUB}, w_{ijUB}$: μ_i', p_j and w_{ij} obtained as the solutions for the UB problem.

Appendix B

System Parameterization with Dissipation Elements

Consider a causal LTI system with n energy storage elements and m dissipation elements. Let $\mu_{ei},\ i = 1,\ldots,n$ be the parameters of the energy storage elements. Let $\mu_{dj},\ j = 1,\ldots,m$ be the parameters of the dissipation elements. The unit of μ_{dj} is either resistance or conductance, depends on the causality of μ_{dj}. Let the state variables be choosen as the generalized momenta associated with the inductances and the generalized displacement associated with the capacitances. The state space equaton of the system can be written as[38],

$$\mathbf{A} = [\mathbf{J}_{SS} + \mathbf{J}_{SL}\mathbf{L}\mathbf{J}_{LS}]\,\mathbf{E} \tag{B.1}$$

$$\mathbf{B} = [\mathbf{J}_{SU} + \mathbf{J}_{SL}\mathbf{L}\mathbf{J}_{LU}] \tag{B.2}$$

$$\mathbf{C} = [\mathbf{J}_{OS} + \mathbf{J}_{OL}\mathbf{L}\mathbf{J}_{LS}]\,\mathbf{E} \tag{B.3}$$

$$\mathbf{D} = [\mathbf{J}_{OL}\mathbf{L}\mathbf{J}_{LU}] \tag{B.4}$$

where,

$$\mathbf{E} = \begin{bmatrix} \frac{1}{\mu_{e1}} & & \\ & \ddots & \\ & & \frac{1}{\mu_{en}} \end{bmatrix} \tag{B.5}$$

$$\mathbf{L} = \begin{bmatrix} \mu_{d1} & & \\ & \ddots & \\ & & \mu_{dm} \end{bmatrix} \tag{B.6}$$

and all $\mathbf{J}$ matrices are determined by system structure and are independent of μ_{ei} and μ_{dj}. So the state space representation contains multiplication of μ_{ei} and μ_{dj}.

Substitute $\mathbf{A}$, $\mathbf{B}$, $\mathbf{C}$ and $\mathbf{D}$ into positive definite lemma, i.e. Inequality (4.17) one gets the condition μ_{ei} and μ_{dj} shall satisfy. The inequality contains the term $\mathbf{PA} + \mathbf{A}^*\mathbf{P}$. According to Equation (B.1) one has,

$$\mathbf{PA} = \mathbf{P}\left[\mathbf{J}_{ss} + \mathbf{J}_{SL}\mathbf{L}\mathbf{J}_{LS}\right]\mathbf{E} \tag{B.7}$$

The right hand side of Equation (B.7) contains the multiplications of three undetermined variables, which are the components of $\mathbf{P}$, $\mathbf{L}$ and $\mathbf{E}$. Thus the resultant constraint is a 'tri-linear' inequality.

Appendix C

State Space Realization of Error Model with Input and Output Filters

Now let us construct a state space realization of the error model with input and output filters. This system is a series connectoin of the input filter, the error model without filters and the output filter. Let a state space realization of the input filter be $\mathbf{A}_{in}$, $\mathbf{B}_{in}$, $\mathbf{C}_{in}$ and $\mathbf{D}_{in}$. Let the state space realization of the output filter be $\mathbf{A}_{out}$, $\mathbf{B}_{out}$, $\mathbf{C}_{out}$ and $\mathbf{D}_{out}$. An the state space realization of the error model, according to Equation (4.18),

$$\mathbf{A}_{error0} = \begin{bmatrix} \mathbf{A} & \mathbf{0} \\ \mathbf{0} & \mathbf{A}_g \end{bmatrix} \tag{C.1}$$

$$\mathbf{B}_{error0} = \begin{bmatrix} \mathbf{B} \\ \mathbf{B} \end{bmatrix} \tag{C.2}$$

$$\mathbf{C} = \begin{bmatrix} \mathbf{C}_{error0} & -\mathbf{C}_g \end{bmatrix} \tag{C.3}$$

$$\mathbf{D} - \mathbf{D} = \mathbf{0} \tag{C.4}$$

Denote the inputs and the outputs of the input filter, the error model without filter and the output filter be $\mathbf{u}_{in}$, $\mathbf{y}_{in}$, $\mathbf{u}_{error0}$, $\mathbf{y}_{error0}$, $\mathbf{u}_{out}$ and $\mathbf{y}_{out}$ respectively. Also

denote the corresponding state vectors be $\mathbf{x}_{in}$, $\mathbf{x}_{error0}$ and $\mathbf{x}_{out}$ respectively. Note that $\mathbf{y}_{out}$ is also the output of the overall system and $\mathbf{u}_{in}$ is also the input to the overall system. Let us first look at the output filter, which can be represented as,

$$\frac{d}{dt}\mathbf{x}_{out} = \mathbf{A}_{out}\mathbf{x}_{out} + \mathbf{B}_{out}\mathbf{u}_{out} \tag{C.5}$$

$$\mathbf{y}_{out} = \mathbf{C}_{out}\mathbf{x}_{out} + \mathbf{D}_{out}\mathbf{u}_{out} \tag{C.6}$$

Due to the series connection between the error model without filters and the output filter, $\mathbf{u}_{out}$ is in fact $\mathbf{y}_{error0}$. Also $\mathbf{y}_{error0}$ can be written as,

$$\mathbf{y} = \mathbf{C}_{error0}\mathbf{x}_{error0} \tag{C.7}$$

Substitute Equation (C.7) into Equations (C.5) and (C.6) one gets,

$$\frac{d}{dt}\mathbf{x}_{out} = \mathbf{A}_{out}\mathbf{x}_{out} + \mathbf{B}_{out}\mathbf{C}_{error0}\mathbf{x}_{error0} \tag{C.8}$$

$$\mathbf{y}_{out} = \mathbf{C}_{out}\mathbf{x}_{out} + \mathbf{D}_{out}\mathbf{C}_{error0}\mathbf{x}_{error0} \tag{C.9}$$

With the state space representation of the error model of,

$$\frac{d}{dt}\mathbf{x}_{error0} = \mathbf{A}_{error0}\mathbf{x}_{error0} + \mathbf{B}_{error0}\mathbf{u}_{error0} \tag{C.10}$$

$$\mathbf{y}_{error0} = \mathbf{C}_{error0}\mathbf{x}_{error0} \tag{C.11}$$

one can rewrite Equations (C.8) and (C.9) as,

$$\frac{d}{dt}\begin{bmatrix} \mathbf{x}_{out} \\ \mathbf{x}_{error0} \end{bmatrix} = \begin{bmatrix} \mathbf{A}_{out} & \mathbf{B}_{out}\mathbf{C}_{error0} \\ \mathbf{0} & \mathbf{A}_{error0} \end{bmatrix}\begin{bmatrix} \mathbf{x}_{out} \\ \mathbf{x}_{error0} \end{bmatrix} + \begin{bmatrix} \mathbf{0} \\ \mathbf{B}_{error0} \end{bmatrix}\mathbf{u}_{error0} \tag{C.12}$$

$$\mathbf{y}_{out} = \begin{bmatrix} \mathbf{C}_{out} & \mathbf{D}_{out}\mathbf{C}_{error0} \end{bmatrix}\begin{bmatrix} \mathbf{x}_{out} \\ \mathbf{x}_{error0} \end{bmatrix} \tag{C.13}$$

Due to the series connection between the input filter and the error model without the filter, one has $\mathbf{u}_{error0} = \mathbf{y}_{in}$. Therefore one has the equation,

$$\frac{d}{dt}\begin{bmatrix} \mathbf{x}_{out} \\ \mathbf{x}_{error0} \end{bmatrix} = \begin{bmatrix} \mathbf{A}_{out} & \mathbf{B}_{out}\mathbf{C}_{error0} \\ \mathbf{0} & \mathbf{A}_{error0} \end{bmatrix}\begin{bmatrix} \mathbf{x}_{out} \\ \mathbf{x}_{error0} \end{bmatrix} + \begin{bmatrix} \mathbf{0} \\ \mathbf{B}_{error0} \end{bmatrix}\mathbf{y}_{in} \tag{C.14}$$

$$\mathbf{y}_{out} = \begin{bmatrix} \mathbf{C}_{out} & \mathbf{D}_{out}\mathbf{C}_{error0} \end{bmatrix}\begin{bmatrix} \mathbf{x}_{out} \\ \mathbf{x}_{error0} \end{bmatrix} \tag{C.15}$$

where $\mathbf{y}_{in}$ is determined by the following equation,

$$\frac{d}{dt}\mathbf{x}_{in} = \mathbf{A}_{in}\mathbf{x}_{in} + \mathbf{B}_{in}\mathbf{u}_{in} \tag{C.16}$$

$$\mathbf{y}_{in} = \mathbf{C}_{in}\mathbf{x}_{in} + \mathbf{D}_{in}\mathbf{u}_{in} \tag{C.17}$$

Substitute Equations (C.16) and (C.17) into Equations (C.14) and (C.15) one gets,

$$\frac{d}{dt}\begin{bmatrix} \mathbf{x}_{in} \\ \mathbf{x}_{out} \\ \mathbf{x}_{error0} \end{bmatrix} = \begin{bmatrix} \mathbf{A}_{in} & \mathbf{0} & \mathbf{0} \\ \mathbf{0} & \mathbf{A}_{out} & \mathbf{B}_{out}\mathbf{C}_{error0} \\ \mathbf{B}_{error0}\mathbf{C}_{in} & \mathbf{0} & \mathbf{A}_{error0} \end{bmatrix}\begin{bmatrix} \mathbf{x}_{in} \\ \mathbf{x}_{out} \\ \mathbf{x}_{error0} \end{bmatrix} + \begin{bmatrix} \mathbf{B}_{in} \\ \mathbf{0} \\ \mathbf{B}_{error0}\mathbf{D}_{in} \end{bmatrix}\mathbf{u}_{in} \tag{C.18}$$

$$\mathbf{y}_{out} = \begin{bmatrix} \mathbf{0} & \mathbf{C}_{out} & \mathbf{D}_{out}\mathbf{C}_{error0} \end{bmatrix}\begin{bmatrix} \mathbf{x}_{in} \\ \mathbf{x}_{out} \\ \mathbf{x}_{error0} \end{bmatrix} \tag{C.19}$$

Substitute Equations (C.1) through (C.3) one gets Equation (4.25) immediately.

Bibliography

[1] Ye, Y. and Youcef-Toumi, K., "Model Reduction in Physical Domain", *Proceedings of American Control Conference 1999*, San Diego, CA, 1999, pp 4486-4490

[2] Ye, Y. and Youcef-Toumi, K., *Eigenvalue Synthesis of Interconnected Systems*, Proceedings of the American Control Conference, vol. 6, pp 4486 - 4490, Chicago, IL, 2000

[3] Ye, Y. and Youcef-Toumi, K., *Contribution to Eigenvalues of LTI System by Physical Subsystems*, Proceedings on the 2000 ASME International Mechanical Engineering Congress and Exposition, pp. 825 - 830, Orlando, FL., 2000

[4] , Ye, Y. and Youcef-Toumi, K., *Subsystem's Influence on a System Eigenvalue* Proceedings of the IEEE SoutheastCon, Nashville, TN. pp. 261 - 267, 2000

[5] Ye, Y. and Youcef-Toumi, K., *Model Reduction with Physical Interpretation: A Phasor Analysis Approach*, Simulation Series, vol. 31, no. 1, pp. 39 - 44, 1999

[6] Ye, Y. and Youcef-Toumi, K., *Automated Zero Dynamics Derivation From Bond Graph Models*, Simulation Series, vol. 31, no. 1, pp. 143 - 148, 1999

[7] Sharon, A., Hogan, N. and Hardt, D., "Controller Design in the Physical Domain", *Journal of the Franklin Institute*, Vol. 328, No. 5/6, pp 697 - 721, 1991

[8] Huang, S. 1997. *Structural Analysis from System Configurations for Modeling and Design of Multi-Energy Domain Dynamic Systems*, Ph.D thesis, Mechanical Engineering Department, MIT

[9] Huang, S. and Youcef-Toumi, K. *Structural Analysis for Modeling and Design of Multi-Energy Domain Dynamic Systems*, Proceedings of the 1997 1st IEEE/ASME International Conference on Advanced Intelligent Mechatronics, AIM'97. 0155, 1997.

[10] R. DeCarlo and R. Saeks, *Interconnected Dynamical Systems*, Marcel Dekker Inc., New York, 1981

[11] G. Robertson and I. Cameron, *Analysis of dynamic process models for structural insight and model reduction – Part 1. Structural identification measures*, Computers chem. Engng, Vol. 21, No. 5, 1997, pp. 445 - 473

[12] Orbak, A., 1998. *Physical Domain Model Reduction for Design and Control of Engineering Systems*, Mechanical Engineer Thesis, Massachusetts Institute of Technology

[13] Orbak, A., Youcef-Toumi, K. and Sanga, M. *Model Reduction and Design of a Power Steering System* , Proceedings of the American Control Conference. vol. 2, pp. 867-871, 2000.

[14] Bishop, R. *Modern Control Systems Analysis and Design Using MATLAB and SIMULINK*, Addison Wesley Longman, Inc. 1996

[15] Karnopp, D., Margolis, D. and Rosenberg, R. *System Dynamics: A Unified Approach*, New York, NY, Wiley, 1990

[16] Slotine, J. and Li, W. *Applied Nonlinear Control*, Prentice-Hall Inc, Englewood Cliff, NJ., 1991.

[17] Skogestad, S. *Multivariable Feedback Control*, John Willey & Sons, New York, NY., 1996.

[18] Rosenberg, R. and Zhou, T., " Power-Based Model Insight", *Proceedings of the 1988 ASME Winter Annual Meeting, Symposium on Automated Modeling for Design*, Chicago, IL, 1988, pp61-67

[19] Resenberg, R. and Ermer, G., 1995, *A Bond Graph Visualization Tool to Improve Engineering System Design*, Systems Analysis, Modeling, Simulation, Vol. 18-19, pp 173

[20] J. Ferris, J. Stein and M. Bernitsas, *Development of Proper Models of Hybrid Systes*, Proceedings of the 1994 ASME International Mechanical Engineering Congress and Exposition - Dynamic Systems and Control Division, Symposium on Automated Modeling: Model Synthesis Algorithms, pp. 629-636, November, Chicago, IL.

[21] Wilson, B. H. and Stein, J. L., "An Algorithm for Obtaining Proper Models of Distributed and Discrete Systems" *Transactions of the ASME, Journal of Dynamic Systems, Measurement and Control*, Vol. 117, No. 4, pp. 534-540, 1995

[22] D.G. Walker, J.L. Stein and A.G. Ulsoy, *An Input-Output Criterion for Linear Model Deduction*, Proceedings of the 1996 ASME International Mechanical Engineering Congress and Exposition - Dynamic Systems and Control Division, Symposium on Automated Modeling, November, Atlanta, GA.

[23] Stein, J and Loucas, L, *Template-Based Modeling Approach for System Design: Theory and Implementation*, Transactions of the Society for Computer Simulation. v 13 n 2 Jun 1996. p 87-101.

[24] Louca, L., Stein, J., Hulbert, G., and Sprague, J., 1997. *Proper Model Generation: An Energy-Based Methodology*, Proceedings of ICBGM'97, 3rd International Conference on Bond Graph Modeling and Simulation, Phoenix, AZ.

[25] J. Ferris, J. Stein and M. Bernitsas, *Development of Proper Models of Hybrid Systems*, Journal of Dynamic Systems, Measurement, and Control. Paper No. GT95-185. 1998.

[26] Louca, L. and Stein, J., *Energy Based Model Reduction of Linear Systems*, International Conference on Bond Graph Modeling, San Francisco, CA 1999

[27] Beck, C., Doyle, J. and Glover, K., *Model reduction of multidimensional and uncertain systems*, IEEE Transaction on Automatic Control, vol. 41, no. 10, pp. 1466 - 1477, 1996

[28] Beck, C. and Doyle, J. *Model reduction of behavioral systems*, Proceedings of the 32nd IEEE Conference on Decision and Control, vol. 4, pp. 3652 -3657, 1993

[29] Wang, W., Doyle, J., Beck, C. and Glover, K., *Model reduction of LFT systems* Proceedings of the 30th IEEE Conference on Decision and Control, vol. 2, pp. 1233 -1238, 1991

[30] Bendotti, P. and Beck, C.L. *On the role of LFT model reduction methods in robust controller synthesis for a pressurized water reactor* , IEEE Transactions on Control Systems Technology, vol. 7, no. 2, pp. 248 -257, 1999

[31] Lall, S. and Beck, C. *Model Reduction of Complex Systems in the Linear-Fractional Framework*, Proceedings of the 1999 IEEE International Symposium on Computer Aided Control System Design, pp. 34 - 39, 1999

[32] Beck, C. and Bendottii, P. *Model reduction methods for unstable uncertain systems*, Proceedings of the 36th IEEE Conference on Decision and Control, vol. 4, 1997

[33] K. Zhou, J. Doyle *Essentials of Robust Control*, Prentice-Hall Inc., NJ, 1998

[34] Helmesson, A., *Model Reduction Using LMIs*, Proceedings of the 33rd Conference on Decision and Control, Lake Buena Vista, FL. 1994

[35] Vasca, F. and Verghese, G. *Adimensional Models and Participation Factors for the Analysis of Induction Motor Dynamics*, Proceedings of the IEEE International Symposium on Industrial Electronics, vol. 2, pp. 480 - 485, 1999.

[36] Balabanian, N. and Bickart, T., *Linear Network Theory*, Matrix Publishers Inc., Beaverton, OR 1982

[37] Fikhtengolts, G. *The Fundamentals of Mathematical Analysis* Pergamon Press, New York, NY., 1965

[38] R. Rosenberg, *State-Space Formulation for Bond Graph Models of Multiport Systems*, Journal of Dynamic Systems, Measurement and Control, March, 1971

[39] Fukuda, M. and Kojima, M., *Branch-and-Cut Algorithms for the Bilinear Matrix Inequality Eigenvalue Problem*, Computational Optimization and Applications, vol. 19, pp. 79-105, 2001

[40] Tuan, H. and Akparian, P., *Low Nonconvexity-Rank Bilinear Matrix Inequalities: Algorithm and Applications in Robust Controller and Structure Designs*, IEEE Transaction on Automatic Control, vol. 45, no. 11, pp. 2111 - 2117, 2000

[41] Fukuda, M. and Kojima, M., *Branch-and-Cut Algorithms for the Bilinear Matrix Inequality Eigenvalue Problem*, Research Report on Mathematical and Computing Science, Series B: Operations Research, Department of Mathematical and Computing Science, Tokyo Institute of Technology, 1999.

[42] Tuan, H., Akparian, P. and Nakashima, Y., *A New Lagrangian Dual Global Optimization Problem for Solving Bilinear Matrix Inequalities*, Proceedings of the American Control Conference, San Diego, CA. pp. 1851 - 1855, 1999

[43] Yamada, Y. and Hara, S., *Matrix-Based Bounding vs. Element-Wise Bounding for the MPEP Global Optimization*, Proceedings of the 37th IEEE Conference on Decision and Control, Tampa, FL., pp. 3861 - 3866, 1998

[44] Fujioka, H. and Hoshijima, K. *Bounds for BMI Eigenvalue Problems - A Good Lower Bound and a Cheap Upper Bound*, Transactions of the Society of Instrument and Control Engineers, vol. 33, pp. 616 - 621, 1997.

[45] Beran, E., Vandenberge, L. and Boyd, S., *A Global BMI Algorithm based on the Generalized Benders Decomposition* Proceedings of the European Control Conference, 1997.

[46] O. Toker and H. Ozbay, *On the NP-Hardness of Solving Bilinear Matrix Inequality and Simultaneous Stabilization with Static Output Feedback*, Proceedings of the American Control Conference, pp 2525 - 2526, 1995

[47] Goh, K., Safonov, G. and Papavassilopoulos, G., *A Global Optimization Approach for the BMI Problems*, Proceedings of the 33rd Conference on Decision and Control, pp. 2009 - 2014, Lake Buena Vista, FL. 1994

[48] Goh, K., Turan, L. and Safonov, G., *Biaffine Matrix Inequality Properties and Computational Methods*, Proceedings of the American Control Conference, pp. 850 - 855, Baltimore, MD. 1994

[49] Horst, R. and Tuy, H., *Global Optimization: Deterministic Approaches*, Springer-Verlag Berlin, 1996

[50] Miller, R., *Optimization: Foundations and Applications*, John Willey & Sons Inc., 2000

[51] Reffield, R. *Dynamic System Synthesis with a Bond Graph Approach: Part II - Conceptual Design of an Inertial Velocity Indicator*, Journal of Dynamic Systems Measurement & Control-Transactions of the ASME. vol. 115, no 3, Sep 1993. pp. 364-369.

[52] Redfield, R. and Krishnan, S. *Dynamic System Synthesis with a Bond Graph Approach: Part I - Synthesis of One-Port Impedances* Journal of Dynamic Systems Measurement & Control-Transactions of the ASME. vol. 115, no. 3, Sep 1993. pp. 357-363

[53] Redfield, R. *Bond Graphs in Dynamic Systems Design: Concepts for a Continuously Variable Transmission*, Simulation Series, vol 31, no. 1, 1999

[54] Connolly, T. and Longoria, R., *Simulation-Based Synthesis for Engineering Systems that Contain Active Elements*, Proceedings of the ASME Dynamics and Control Division - 2000, vol. 2., pp 831 - 838

[55] Asada, H., Gordon, B. and Gu, B., "A Unified Approach to Modeling and Realization of Constraint Robot Motion Using Singularly Perturbed Sliding Manifolds," *Proceedings of the IEEE International Conference on Robotics and Automation*, San Francisco, CA, 2000

[56] Brandon, G. Liu, S. and Asada, H., "Realization of High Index Differential-Algebraic Systems using Singularity Perturbed Sliding Manifolds" *Proceedings of the American Control Conference 2000*, Chicago, IL, 2000, pp752 - 756

[57] Wang, W., Doyle, J., Beck, C. and Glover, K., "Model Reduction of LFT Systems", *Proceedings of the 30th Conference on Decision and Control*, Brighton, England, 1991, pp 1233 - 1238

[58] Beck, C., Doyle, J. and Glover, K., "Model Reduction of Multidimensional and Uncertain Systems", *IEEE Transaction on Automated Control*, Vol. 41, No. 10, pp 1466 - 1477, 1996

[59] Fortuna, L., Nunnari, G. and Gallo, A., *Model Order Reduction Techniques with Applications in Electrical Engineering*, London, England, Srpinger-Verlag, 1992

[60] Megretski, A., 2000 *6.245: Multivariable Control Systems*, Department of Electronic Engineering and Computer Science, MIT, 2000